JOM
https://doi.org/10.1007/s11837-021-04872-y

TECHNICAL ARTICLE

Oxidation in Reused Powder Bed Fusion Additive Manufacturing Ti-6Al-4V Feedstock: A Brief Review

NICHOLAS DERIMOW [1,2] and NIKOLAS HRABE[1,3]

1.—Applied Chemicals and Materials Division, NIST, Boulder, CO 80305, USA. 2.—e-mail: nicholas.derimow@nist.gov. 3.—e-mail: nik.hrabe@nist.gov

Unmelted titanium alloy (Ti-6Al-4V) feedstock powder oxidizes during powder bed fusion additive manufacturing. This review focuses on the potential effect variations of the powder reuse method may have on the oxidation rate over multiple builds in both electron beam and laser powder bed fusion processes. No correlation of the oxidation rate based on the powder reuse method has been observed, but significant variation in the oxidation rate has been observed between reuse methods. The authors feel that these results highlight a need for better reporting of the details of the powder reuse method (e.g., mixing) to appropriately assess the potential for the reuse method to affect the oxidation rate. Recommendations for powder reuse and details for a higher level of reporting are provided. Multiple instances of variable oxidation rate within a given experiment have been observed. The implications of this heterogeneity on mechanical property variability might be significant.

INTRODUCTION

Additive Manufacturing of Titanium

The development of metal additive manufacturing (AM) has brought forth a paradigm shift in the manufacturing of metals and alloys, such that complex metal parts can now be fabricated using computer-aided design (CAD) as opposed to traditional metallurgical methods and extractive manufacturing. AM enables net shape or near-net shape fabrication of parts with complex geometries to be digitally designed and easily printed, thereby cutting down on manufacturing lead times across a wide variety of industries. The constant stream of advances in AM technologies led by governmental, industrial, and academic efforts has given rise to real-world use cases of metal AM parts, ranging from aerospace technology to medical device applications. Due to the advantages of this process, the medical and aerospace industries have invested heavily in AM, mostly in titanium-based alloys due to their high strength-to-weight ratios and corrosion resistance. This, in turn, has propelled the AM community to concentrate its efforts towards the qualification of titanium alloys, mainly the Ti-6Al-4V alloy, for fatigue- and fracture-critical applications. However, AM Ti-6Al-4V has yet to see wide adoption for such applications due to an incomplete understanding of the processing–structure–properties–performance (PSPP) relationships across the many different additive manufacturing technologies, individual machine settings, powder-handling methods, and post-processing treatments.[1] Sales of all AM products and services worldwide are forecast to reach US$35.6 billion in 2024,[2] and therefore a qualification framework and standardization of the processes will provide an enormous beneficial impact on industry needs. One such example includes aerospace part maintenance, repair, and sustainability, as AM of Ti-6Al-4V provides a unique solution for overcoming long lead times for parts with complex geometries in which buy-to-fly ratios tend to be large.[3]

One of the key components when developing a qualification framework for AM Ti-6Al-4V for fatigue- and fracture-resistant applications is to critically understand the effects of oxygen contamination on the AM parts and powder feedstock. Titanium alloys have a high affinity for oxidation

(Received May 5, 2021; accepted August 24, 2021)

Published online: 17 October 2021

due to their high oxygen reactivity at elevated processing temperatures, requiring expensive and elaborate mitigation processes. Traditional titanium metallurgy requires that the processing environments consist of vacuum or inert atmospheres in order to maintain ductility, since the oxygen content is directly related to the increased yield strength (YS) and ultimate tensile strength (UTS) in Ti-alloys, as shown in Fig. 1, with data digitized and replotted from Ref. 4. There is a strength–ductility trade-off with increasing amounts of oxygen present either in the interstitial regions or in the form of oxides. The minimum values for YS and UTS in accordance with ASTM F1472-14 are shown as horizontal dashed lines.[5] It is apparent how small changes in oxygen content can lead to large changes in mechanical properties. In some instances, failure to control the oxygen content can lead to a material that does not meet the material's specification requirements.

The aim of this review is to summarize the literature relating specifically to the reuse of Ti-6Al-4V powder feedstock batches and its subsequent effects on the oxidation and resulting mechanical properties in AM Ti-6Al-4V builds. For other aspects of AM of Ti-6Al-4V and Ti powder metallurgy, the authors direct the interested reader to Table I, where a non-exhaustive list of review studies pertaining to these topics involving Ti-6Al-4V is given. The goal of the present review is not to redundantly describe every aspect of Ti-6Al-4V metallurgy with respect to AM, but rather to fill in the gaps of information with respect to Ti-6Al-4V powder reuse in PBF AM. Other recent reviews not directly pertaining to Ti-6Al-4V are also helpful for understanding focus on qualification and certification,[6] mechanical properties of AM metals,[7] powders for powder bed fusion (PBF),[8] PSPP relationships,[9] feedstock powder degradation,[10] AM of new materials,[11] and spreadability metrics.[12]

With AM Ti-6Al-4V alloys, oxidation can lead to a number of changes in material properties, highlighted in Table II. In traditional Ti-6Al-4V metallurgy, oxygen is an α phase stabilizer and is sometimes purposely added to increase the strength of the alloy. However, oxidation is not always beneficial in additive Ti-6Al-4V. At this stage in AM technology development, oxygen is an uncontrolled contaminant by-product of PBF processes for atmospherically sensitive alloys such as Ti-6Al-4V, through simultaneous exposure to high temperatures and oxygen sources. High background temperatures (400° C–800° C) in electron beam (EB)-PBF exist due to layer preheating, leading to temperatures high enough to sinter any unmelted powder in the entire build area. High temperatures in laser (L)-PBF exist only in close proximity to melted parts and may or may not be high enough to achieve sintering, although they are high enough to increase the oxygen affinity of Ti-6Al-4V and lead to powder oxidation. The assumed main source of oxygen during EB-PBF is thought to be powder moisture.[25] The vast majority of AM machines lead unavoidably to powder exposure to the atmosphere between builds. Due to the small powder (median particle size about 25 μm) and narrow (5–25 μm) size distributions used in PBF AM, the significant

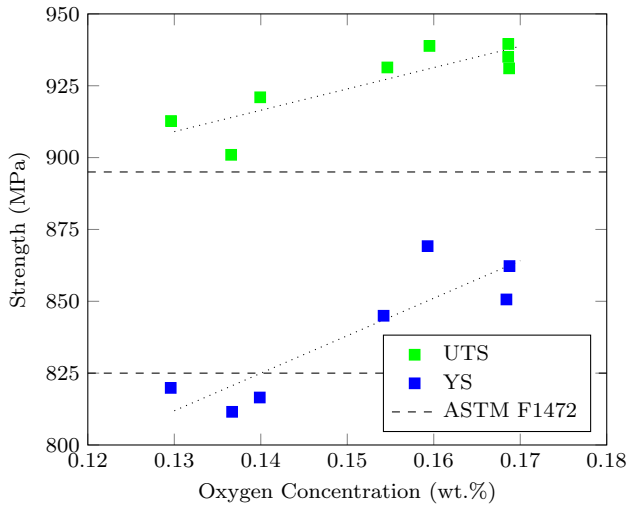

Fig. 1. Tensile properties of wrought Ti-6Al-4V as a function of oxygen content, recreated from Ref. 4. Dashed horizontal lines represent the minimum requirements for UTS and YS in accordance with ASTM F1472-14.

Table I. Non-exhaustive list of reviews pertaining to Ti-6Al-4V

Topic	References
Powder metallurgy	13
Strength and ductility	14
Effects of interstitial solutes	15
Feedstock production	16
Fatigue in AM	17, 18
Mechanical properties	19
Solidification modeling	20
Direct metal laser deposition	21
General overview	22
High oxygen content powder	23
Oxygen effects on ductility	24

Table II. Effects of oxygen in AM Ti-6Al-4V

Topic	References
Reduced impact toughness	26
Increased strength	27–29
Decreased elongation	29, 30
Material embrittlement	31
Decreased fatigue resistance	32
Difference in α/β phase fraction	33
Anisotropy in tensile behavior	34

Table III. Chemical requirements for ASTM F2924-14 (Grade 5) and ASTM F3001-14 (Grade 23, ELI) Ti-6Al-4V for PBF feedstock. Tr. = traceelements; Units are in wt%

ASTM	Al	V	Fe	O	C	N	H	Y	Trace	Trace max.	Ti
F2924	5.5 < x < 6.75	3.5 < x < 4.5	0.30	0.20	0.08	0.05	0.015	0.005	0.10	0.40	bal.
F3001	5.5 < x < 6.50	3.5 < x < 4.5	0.25	0.13	0.08	0.05	0.012	0.005	0.10	0.40	bal.

Table IV. Powder characterization methods adapted from Ref. 38

Technique	Characterization
Helium pycnometry	Particle density
Laser diffraction	Particle size distribution
X-ray computed tomography	Particle size and morphology
X-ray diffraction (XRD)	Crystallographic phases
Scanning electron microscopy (SEM)	Microstructure, morphology, Z-contrast
Transmission electron microscopy	Microstructure, phase identification
Energy-dispersive X-ray spectroscopy (EDS)	Bulk chemical analysis
Gas/liquid/ion chromatography	Bulk chemical analysis
Mass spectroscopy	Bulk chemical analysis
X-ray photoelectron spectroscopy (XPS)	Surface chemical analysis
Combustion analysis (e.g., LECO and Eltra)	Bulk light element analysis C, H, N, O, S)
Atom probe tomography (APT)	Atomic-resolution chemical analysis
Powder trap capsule	AM powder bed density (PBD)[39]

powder surface area attracts moisture quickly and in large quantities when exposed to the atmosphere for even a short time. During the subsequent build, this moisture provides an oxygen source for powder oxidation. An additional potential oxygen source in L-PBF is shielding gas impurities. The shielding gas is used to prevent deleterious interaction of the melt pool vapor plume with the laser or the powder bed. However, a range of shielding gas purity is used, and impurities in that shielding gas could be a source of oxygen during the L-PBF process. EB-PBF has a similar potential additional source of oxygen from helium impurities. EB-PBF is a vacuum process, but helium is introduced into the build chamber throughout the build process to maintain a more consistent vacuum level and improve beam quality and build outcome.

Unwanted oxygen incorporation in each build compounds over multiple builds and decreases the lifetime of the reused feedstock powder, and can lead to the many effects listed in Table II. An important outstanding question in the AM of Ti-6Al-4V is: how does the overall AM process and subsequent powder reuse methods affect the oxidation rate of reused powder batches over multiple builds and subsequent effects in as-built material? These issues have led the AM community to track the oxidation of Ti-6Al-4V feedstock powder oxidation and set allowable quantities for specific use cases.

The current ASTM standard specifications for AM PBF Ti-6Al-4V are ASTM F2924-14[35] pertaining to Grade 5, and ASTM F3001-14[36] for Grade 23, (extra-low interstitials, ELI) Ti-6Al-4V alloy. The values presented in Table III refer to the allowable quantities for each alloying element in the ASTM F2924-14 and F3001-14 standards for Ti-6Al-4V. Of all these elements, oxygen is the most dynamically changing throughout the lifetime of a powder batch. The chemical analysis is typically carried out using inert gas fusion techniques with LECO and Eltra chemical analysis devices*. However, these inert gas fusion techniques do not quantify the form or species of oxide in the powder batch, so that it is not fully known if the oxygen was interstitial or present in the form of a surface metal oxide.

Several powder characterization techniques can be employed for powder characterization, listed in Table IV recreated from Ref. 37. These techniques have all been utilized for the study of Ti-6Al-4V powders. However, many of these techniques can only provide a quantitative representation of the powder oxidation and the relative oxidation of internal phases in singular particles. The higher-resolution techniques for chemical analysis such as scanning transmission–energy-dispersive x-ray spectroscopy (EDS) and atom probe tomography require extremely small sample sizes; therefore, it is difficult to quantitatively assess the oxidation in bulk powder batches of Ti-6Al-4V. However, the focus of this review article is the changes in PBF

*Commercial names are identified in order to adequately specify the experimental procedure. Such identification is not intended to imply recommendation or endorsement by the NIST, and nor does it imply that they are necessarily the best available for the purpose.

titanium powder oxygen content due to powder reuse methods.

Recent investigations into powder atomization highlight the need for a better understanding and improvement of the atomization of feedstock powder used in AM,[37] as various powder characteristics, such as spreadability, flowability, internal porosity, size distribution, tap density, apparent density, chemistry, morphology, and moisture content, can play critical roles in the AM process, especially oxygen-sensitive metals like Ti-6Al-4V.

Powder Handling and Reuse Methods

There are many different ways to reuse powder feedstock in PBF processes, and it can be quite challenging to distinguish exactly which method was employed when reading powder reuse studies. In general, most researchers and AM part manufacturers will seek to reuse leftover metal powder from the powder bed for subsequent builds to maintain the cost effectiveness of the process. However, the method in which they reuse their powder can often be opaque to external institutions and researchers. Throughout this literature survey, there were a number of overlapping methods for powder reuse, and, in order to categorize these methods as accurately as possible, a non-exhaustive classification system was developed for the purposes of this review in order to present the data as concisely as possible. Note that the developed classification system does not reflect all the ways Ti-6Al-4V powder can be reused, but rather those that were observed from the literature at hand. Individual Ti-6Al-4V part manufacturers may have their own proprietary or process-optimized methods for powder reuse, as well as qualified methods for specific part production as per regulating body requirements. The following processes described below only generalize the overall type of powder reuse schema, and may lack specific details that were unfortunately not present in the literature. The description of these processes in this work are only general and may lack specific details that were unfortunately not present in the literature.

The flow chart presented in Fig. 2 describes a generalized powder reuse flow encompassing the methods used in the literature. The arrows indicate the flow of progression from each step, and only specifically to a certain process when denoted as such. The powder reuse processes are referred to as Processes A, B, C, and D, labeled in Fig. 2. The dashed line represents a flow that is only performed when the entire lot has been through the machine at least once.

– **Process A** describes a powder reuse method that applies to both EB-PBF and L-PBF such that no virgin powder is added, and the leftover powder in the build area for a given build is sieved and possibly mixed followed by reintroduction into the powder hoppers or feed regions for subsequent builds. This leads to an overall loss in volume of the powder, and this process is carried out until there is no longer enough powder left to complete the builds. Due to a lack of specific information in the literature, there is uncertainty with respect to the handling of the remaining powder sitting in the hoppers/feed regions. Specific details are missing as to whether this powder will be mixed with the build area powder, followed by reintroduction to the hoppers/feed regions, or if the build area powders are recombined and added on top of the unused hopper powder or feed regions.
– **Process B** describes a schema such that virgin powder is added to every build in order to make up for the mass loss due to part fabrication. Like Process A, there exists uncertainty as to whether virgin and build area powder are mixed with each other, and/or the hopper/feed region powder, or just added to the top of the remaining hopper/feed region powder.

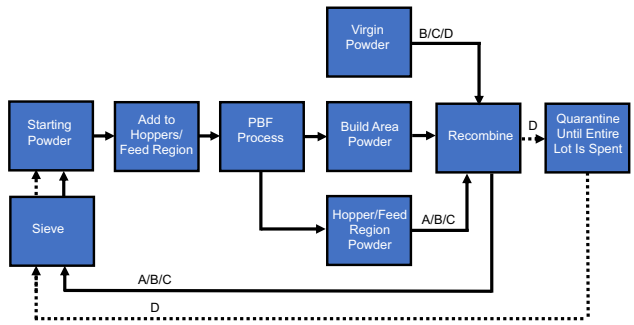

Fig. 2. Generalized powder reuse schema as employed by the work cited in this review.

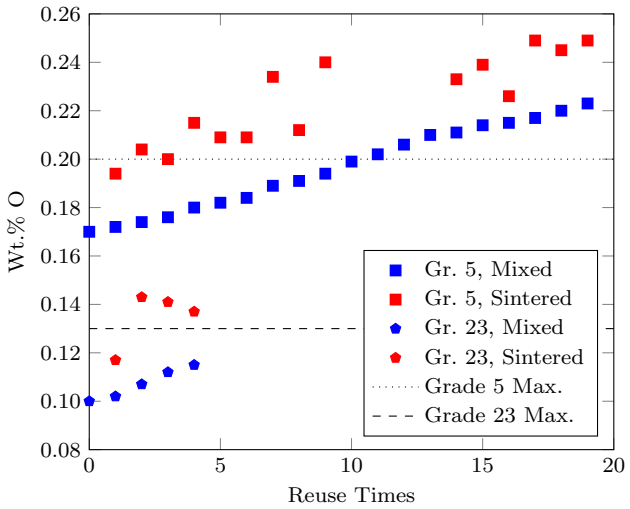

Fig. 3. Oxygen pickup in Grade 5 Ti-6Al-4V powder adapted from Ref. 25. Sintered powder taken only from the sintered cake; Mixed powder that was reused according to Process A (mixing of the sintered powder with remaining powder in the hoppers).

- **Process C** describes a schema that incorporates both Processes A and B, such that no virgin powder is added until after a specific cycle, N. This process could then be repeated, adding or 'refreshing' powder batches with virgin powder on an as-needed basis. Again, it is unclear whether some combination of virgin, build area, and hopper/feed region powder is mixed with each other or just added separately to the hoppers/feed regions.
- **Process D** describes Arcam's recommended powder reuse schema for their EB-PBF machines. This process involves a quarantining of used powder such that all the starting/virgin powder has gone through the machine at least once, so that the quarantined powder batches have all seen the same number of builds and have been refreshed with equal amounts of virgin powder to make up for loss of mass. Once all the starting powder has been depleted, the quarantined powder becomes the new starting powder. Although this is Arcam's recommended procedure, there may exist slight differences in the procedure across Arcam machine users.

SUMMARY OF POWDER REUSE STUDIES

The following sections are summaries of Ti-6Al-4V specific powder reuse studies pertaining to the oxidation of the powder and the effects on material properties during EB-PBF and L-PBF AM. Summary tables and graphs for the following sections can be found in Table V and Figs. 6 and 10 (see below) for EB-PBF and Table VI and Figs. 7 and 10 (see below) for L-PBF. To accurately represent the following literature, it must be noted that some of the articles pertaining to Ti-6Al-4V powder reuse did not specifically aim to study the reused powder and only included the oxidation information for completeness. Therefore, as much information as possible was collected regarding oxidation from the literature cited below. However, the entire articles in many cases have not been fully summarized with respect to the entire scope of the individual authors' work, only the portions of the articles pertaining to powder reuse.

Electron Beam Powder Bed Fusion (EB-PBF)

The effects of Ti-6Al-4V powder reuse in the EB-PBF process were initially cataloged in a 2009 internal report by Arcam scientist, Mattias Svensson, where the objectives of the overall experiments were to measure the material properties of EB-PBF Ti-6Al-4V in the as-built state and after hot isostatic pressing (HIP).[25] The aim of the study was to test the as-built and HIPed Ti-6Al-4V (Grade 5) and Ti-6Al-4V ELI (Grade 23) in accordance with the following industrially relevant standards AMS 4999,[40] ASTM F136-08,[41] ASTM F1472-08,[42]and ASTM F1108-04[43] (the latter three of which have since been superseded by ASTM F136-13,[44] ASTM F1472-14,[5] and ASTM F1108-14[45]). The builds were conducted on an Arcam S12 machine in a partial vacuum of He of 2×10^{-3} mbar. Chemical analysis was carried out by a ISO 17025[46] compliant third party laboratory. The virgin powder oxygen content for both the Grade 5 and Grade 23 were measured to be 0.17 wt% O and 0.10 wt% O, respectively. The increasing number of powder reuse times resulted in a steady increase of oxygen pickup, which Svensson stated only occurred during the preheating/sintering stage of the EB-PBF process. Svensson also stated that the oxygen pickup is dependent on the partial pressure of hydrogen in the chamber, but could also be attributable to the powder feedstock morphology, noting that gas-atomized powder had higher increases in oxygen from reuse than plasma-atomized powder. A total of 19 builds were carried out on the Grade 5 powder which resulted in an average oxygen pickup from 0.17 wt% O to 0.22 wt% O of the powder after the remaining powder had been mixed with the powder recovered from the

Table V. List of reuse processes and oxidation in EB-PBF; lengths in parenthesis refer to oxide scale growth

Method	Machine	Reuses #	O_I (wt%)	O_f (wt%)	Ref.
A	S12	26	0.17	0.22	25
A	S12	5	0.10	0.115	25
A	S400	40	0.13	< 0.50	47
D	A1	90	0.14	0.33	48
A	A2	11	0.14	0.20	49
D	–	–	–	–	50
A	A2	21	0.08	0.19	27
A	A2	5	0.138	0.182	59
A	A2X	30	0.15	0.205	64
D	A2X	69	0.124	0.324	29
B	Q10plus	7	0.12	0.15	62
A	Q10plus	10	(6.5 nm)	(7.54 nm)	68
A	A2X	2	0.13	0.17	69
A	A2X	30	0.142	0.356	70–72

sintered cake, in what appears to be a Process A method of powder reuse. The oxygen content of purely the sintered cake increased from 0.17 wt% to 0.195 wt% O after one build, and by build 19 had increased to 0.25 wt% O. The data for these measurements have been replotted from Ref. 25 in Fig. 3. The red data markers in Fig. 3 pertain to the oxygen concentration of the powder collected from the sintered block of material after one build. The blue data markers represent the mixed powder batch of all the leftover material from the process. The average oxygen pickup from the Grade 5 sintered powder from the oxygen content of the feedstock per individual build is calculated to be ≈ 0.03 wt% O/build, while the overall average oxygen pickup rate per build from via mixing the powder was ≈ 0.003 wt% O/build. A total of 5 builds were carried out using the Grade 23 powder, where the average oxygen increase per build never exceeded the 0.13 wt% Grade 23 limit. Measurements of purely sintered cake powder after the first build saw an increase from 0.10 wt%, ultimately increasing to ≈ 0.14 wt% O. The average oxygen pickup rate of the sintered powder from the feedstock is calculated to be 0.029 wt% O/build. The average increase per build after mixing is lower, calculated to be 0.004 wt% O/build. There was a marked decrease in Al content from the powder to the as-built specimen. The tensile properties for both HIPed and as-built samples are maintained through the EB-PBF process. Increased porosity in the as-built specimens led to reduced fracture toughness and rotating bend fatigue life. Svensson concludes that increased oxygen content is dependent on the residual water pressure in the chamber.[25]

One of the first published instances of the effects of reused titanium powder for EB-PBF was in an article by Gaytan et al. in 2009 where the authors investigated the optimization of the EB-PBF build parameters and subsequent effects of such on the microstructure and mechanical properties of mesh structures.[47] The EB-PBF was carried out using 30-μm-diameter Grade 23 Ti-6Al-4V powder on an Arcam EBM S400 machine. The preheated step was carried out with raster beam scans of 15,000 mm/s at a beam current of approximately 30 mA to heat each layer to 640 °C. The melt scan parameters were a 400 mm/s raster speed with 6 mA of beam current and the energy density of the beam was 10^2 kW/cm^2. The build chamber nominal vacuum of 1.3×10^{-4} mbar was increased to 1.3×10^{-2} mbar with a He bleed. The unmelted powder was then mixed with the recovered powder that loosely adhered to the finished part and used for the following build (Process A). This process was carried out 40 times, with analysis of the powder via EDS revealing a decline in Al content and no change in V. The authors note that the detection of less than 0.50 wt% O via EDS was not feasible for the study, and therefore the authors concluded with the reasonable assumption that the oxidation of the reused powder did not exceed the 0.50 wt% O detection limit of the EDS detector. The authors did note that there was a 10–15% reduction in Al in the chemistry of the as-built part. The powder size distribution ranged from a few micrometers to ∼ 100 μm, with an average particle size of about 30 μm.

A general study on the morphology of Ti-6Al-4V powders used in EB-PBF was carried out in 2014 by Mohammadhosseini et al., where the emphasis of the investigation was on the particle size distribution, morphology, and flowability of the powders used in EB-PBF.[48] The authors categorized the oxygen content of the reused powder via inert gas fusion. The average particle size had a median diameter of 67 μm, with a narrow distribution range. The starting oxygen content was measured to be 0.14 wt% O. The reuse procedure consisted of recovering the sintered powder using the Arcam PRS to blast the residual powder off the part, followed by sieving. After corresponding with the authors for this specific study, it was determined that the powder reuse was in accordance with Arcam's recommended procedure (Process D). Mohammadhosseini et al. noted that there were no observable effects in flowability or apparent density in the powder after 90 builds and 1000 h of running the EBM machine. Overall oxygen content was found to increase to 0.33 wt% O after the 90 builds.[48] The authors do not state how large the builds were, but the average amount inferred from the stated 90 builds at 1000 h yields an approximate 11 h/build.

The effects of reuse on EBM Ti-6Al-4V powder were revisited in 2015 with three independent articles by Petrovic et al.,[49] Strondl et al.,[50] and Tang et al.[27] The study by Petrovic et al. was an effort to identify the level of reusability of Ti-6Al-4V powder used in EB-PBF such that it conformed to the aeronautical manufacturing standard for Ti-6Al-4V alloy in sheet, strip, and plate form for then SAE International standard AMS 4911N,[51] which has since been revised in 2019 to AMS 4911R.[52] The study consisted of 16 builds on an Arcam A2 machine with Ti-6Al-4V powder provided by Arcam. The authors did not provide machine settings used for the builds in this experiment, but noted that the preheat temperature of 650°C was achieved and maintained throughout the build. The amount of powder was selected such that the exact number of 16 builds could be achieved, with just enough powder left in the hoppers to maintain powder flow during the build. The powder reuse procedure consisted of blasting off the sintered powder stuck to the as-built part in the PRS and vacuuming loose powder from the build chamber and hoppers to be sieved and reintroduced back into the hoppers (Process A). The authors noted that the procedure was carried out with controlled room temperatures of 21°C–23°C, with a controlled humidity of 35–40%[49]. The chemical analysis of the powder was

carried out in accordance with ASTM E1941-10,[53] ASTM E1447-09,[54] ASTM E1409-13,[55] and ASTM E2371-13[56] for C, H, O/N, and the remaining elements, respectively. Similarly to the previous study by Gaytan et al.,[47] chemical analysis by Petrovic et al. revealed negligible change in V concentration but a decrease in Al content with consecutive builds, and remaining chemically within the limits for the AMS 4911R SAE standard. The starting O concentration of 0.14 wt% increased over the 0.20 wt% AMS 4911N limit after 11 builds (10 powder reuses). The PSD remained in the 45 μm to 110 μm range throughout the builds, and there were no significant morphological differences in the reused powder or microstructural differences in the as-built state visible via scanning electron microscopy. Tensile tests were carried out on samples manufactured in both the horizontal and vertical build directions, where it was noticed that the horizontally built specimens had lower residual strain likely due to the grain orientation from the build direction. The authors note that elongation remained in compliance with the AMS 4911N standard. Petrovic et al. concluded that the established maximum level of reusability in their study was 12 powder reuses, with the limiting chemical change remaining within the standard wt% O. The authors also noted that this study served as a worst-case scenario, as no fresh powder was introduced at any point. Adding fresh powder will lead to better results in reusability.[49]

The work by Strondl et al. focused on the characterization and handling of Ti-6Al-4V powder used in EB-PBF as well as a Ni-alloy powder used for L-PBF.[50] The goal of the investigation was to understand the effects of handling and reuse of the powder on the PSPP relationships in the AM material. The virgin and reused powders from both the EB-PBF and L-PBF processes were evaluated with respect to particle size and morphology via dynamic image analysis, while flow performance was evaluated with a powder rheometer. The reuse procedure for the EB-PBF Ti-6Al-4V powder followed the Arcam standard procedure (Process D). The machine models or melting parameters were not described. The reuse process for the Ni-alloy powder used in L-PBF only involved sieving the powder after the machine use. Chemical analysis was not performed on the EB-PBF Ti-6Al-4V powder. The authors noted that the reused Ti-6Al-4V powder displayed lower flowability, likely due to the coarseness of the reused particles from the blasting process in the PRS.[50]

In the 2015 study by Tang et al., the effect of powder reuse was explicitly studied to investigate the changes in powder composition, particle size distribution, density, flowability, and morphology.[27] Tensile specimens were manufactured in order to correlate the effects of powder reuse with the mechanical properties of the AM parts. The EB-PBF process carried out by Tang et al. involved the use of an Arcam EBM A2 system with beam spot size of 100 μm, layer thickness of 50 μm, and preheating conditions of beam current of 30 mA, scanning speed of 1–1.3 $\times 10^4$ mm/s, and preheat temperature of 730 °C. Layer melting conditions were such that beam current was 20 mA and scanning speed was 4,500 mm/s. The powder used was contained in two 45-kg containers containing a total of 90 kg of Grade 23 Ti-6Al-4V provided by Arcam. The powder capacity of the system enabled 21 powder reuses without introducing any virgin powder (Process A). The AM machine contained a stainless steel substrate that was preheated to 730 °C via electron beam scanning prior to the raking of the first Ti-6Al-4V layer. The authors noted that each layer of powder was preheated to 730 °C, and that the overall temperature of the powder bed never dropped below 550 °C. The reuse process involved blasting the sintered powder off the as-built part in the Arcam Powder Recovery System (PRS), which was mixed with the remaining powder in the PRS

Table VI. List of reuse processes used in L-PBF

Method	Machine	Reuses #	O_I (wt%)	O_f (wt%)	Ref.
A	–	12	–	–	73
A	–	5	0.13	0.13	74
A	Renishaw AM250	38	0.084	0.12	75
C	DMLS	11 (A) + 14 (B)	0.11	0.11	76
A	Concept Laser	10	0.079	0.13	76
A	–	31	0.09	0.11	77
A	EOS M290	15	0.10	0.12	85
B	EOS M290	100	–	–	86
A	SLM Solutions 280	11	0.083	0.08	87
A	EOS M290	8	0.125	0.125[a]	88

[a]Oxygen content of as-built material.

followed by sieving through an 80-mesh (177 μm). Sampling of the powder were taken in accordance with the ASTM B215 powder sampling standard,[57] and powder characterization was performed via atomic emission plasma spectrometry in accordance with ASTM E2371-13[56] for the metallic elements and inert gas fusion for oxides in accordance with ISO 22963:2008.[58] With increased reuse, the PSD became narrower while the morphology of the particles became coarser and less spherical. The powder also had increased flowability. There was a noticeable decrease in Al content from the powder to the as-built part after 21 reuses, with Al content decreasing from 6.35 wt% Al in the powder to 5.93 wt% in the as-built part by the 21st reuse. The concentration of V on the other hand remained relatively unchanged after 21 reuses similar to the previous studies, with a powder to as-built part V content decrease of 0.07 wt%. The authors found that oxygen content had increased over 21 builds from 0.08 wt% O to 0.19 wt% O. This resulted in increased yield and ultimate tensile strengths of the as-built Ti-6Al-4V due the increased oxide strengthening, shown in Fig. 4, with minimal changes in elongation. Tang et al. suggest that the increasing oxidation of the powder occurs when the powder is exposed to air and allowed to retain moisture during the powder reuse recovery stages for reuse. Tang et al. also observed less spherical powder morphology, increased flowability, and a narrower PSD of the reused powder, but consistent tensile properties from builds of various locations on the powder bed (Fig. 5).[27]

A powder reuse study by Nandwana et al. in 2016 investigated Inconel 718 and Ti-6Al-4V powders used in EB-PBF in order to elucidate the factors that determine powder reuse since their was a lack of a standard approach to powder reusability[59] The experiments were carried out using an Arcam A2 system with feedstock powder size distribution ranging from 45 - 105 μm for six builds of Inconel 718 and five builds of Ti-6Al-4V. The builds were conducted with precise amounts of powder such that by the end of the build there would be no powder left in the hoppers. The reuse process therefore consisted of combining the powder from the build chamber with that of the PRS to be sieved and reintroduced into the hoppers (Process A). The vibratory sieve used a 100 mesh (150 μm) screen. Prior to each build, the powder was sampled for chemical analysis. Chemical analysis for the Ti-6Al-4V was performed in accordance with ASTM E1409-13[55] for O/N, ASTM E1941-10[53] for C, ASTM 1447-09[54] for H, and ASTM E2371-13[56] for the remaining elements in the Ti-6Al-4V powder. The Ti-6Al-4V powders saw 175 hours of build time. The authors reported significant metallization of the Arcam A2 heat shields with deposits from the high vapor pressure from the Al in Ti-6Al-4V. The Ti-6Al-4V saw significant oxygen pickup, which ranged from 0.138 wt% to 0.182 wt% in the powder and 0.141 wt% to 0.168 wt% in the build after five builds. The

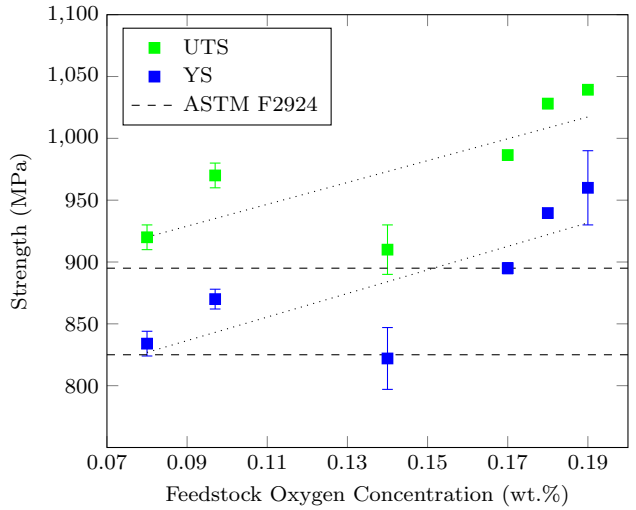

Fig. 4. Tensile properties of EB-PBF Ti-6Al-4V as a function of feedstock oxygen concentration, data plotted from Ref. 27. Dashed horizontal lines represent the minimum requirements for UTS and YS in accordance with ASTM F2924-14.[35]

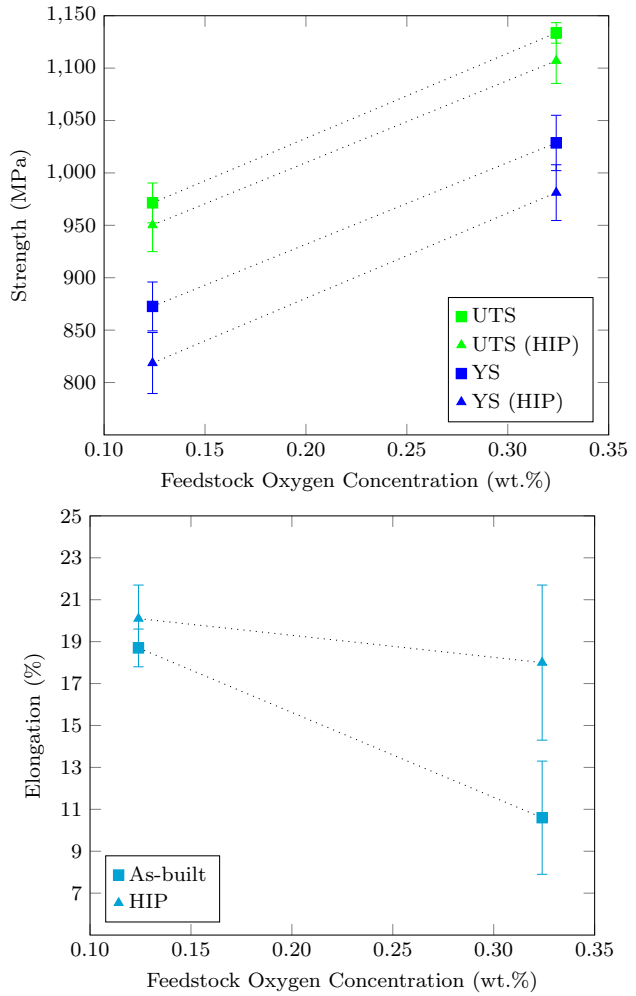

Fig. 5. Tensile properties of EB-PBF Ti-6Al-4V as a function of feedstock oxygen concentration, data plotted from Ref. 29.

authors remark that the governing factors for powder reuse stem from initial powder chemistry and the alloy system itself.[59]

A different approach for investigating increased oxygen content as a function of powder reuse was carried out by Grell et al. in 2017, where the Ti-6Al-4V powder was artificially oxidized to simulate the oxygen uptick from powder reuse in order to study the effects on impact toughness.[26] Building on the work from Tang et al.,[27] Grell et al. sought to investigate the effects of powder oxidation on the impact toughness of Ti-6Al-4V builds at oxygen concentrations significantly higher than the ASTM F2924-14 0.2 wt% O limit for Grade 5 Ti-6Al-4V use in powder bed fusion processes.[35] The artificially oxidized powders were achieved by means of combining low wt% oxygen powder with highly oxidized powder by determining the desired average wt% oxygen via the rule of mixtures. The highly oxidized powder was achieved by subjecting an already 5× reused Ti-6Al-4V powder containing 0.16 wt% O to 650 °C in for 4 h in air. This process increased the oxygen concentration of the powder to 4.1 wt% O, referred to in this review as Powder E. The powder used for these experiments was plasma atomized Ti-6Al-4V, and the feedstock for the builds resulting from the mixtures consisted of:

- Powder A (0.110 wt% O): 100% virgin
- Powder B (0.142 wt% O): 100% 5× reused Powder A
- Powder C (0.340 wt% O): 96.5% Powder B + 3.5% Powder E
- Powder D (0.525 wt% O): 88.8% Powder B + 11.2% Powder E
- Powder E (4.1 wt% O): 100% artificially oxidized in air for 650 °C/4 h

The Charpy specimens were manufactured on separate Arcam A2 and A2X systems with standard Arcam recommended settings with 0.05 mm slice thickness. Hot isostatic pressing (HIP) was carried out on half of the samples for comparison between as-built and HIPed impact energies, with conditions of 100 MPa, 954 °C, and 3 h under inert conditions, followed by cooling below 425 °C. The specimens were machined into 'Type A' Charpy V-notch samples in accordance with ASTM E23-16b[60] (now superseded by ASTM E23-18,[61] where Type A nomenclature has since been replaced by 'V-notch'). The powders were analyzed for oxygen content using inert gas fusion as prescribed in ASTM E1409-13,[55] while the builds were also analyzed via ASTM E1941-10[53] for C, ASTM E1447-09[54] for H, and ASTM E2371-13[56] for the remaining elements. It was found that with increasing oxygen content, the Charpy impact energy decreased from ~ 20 J-50 J 3 J to 5 J as the wt% O of the powder increased from 0.11 wt% to 0.53 wt%. The authors also found that HIP post-processing increased the impact energy of the samples containing up to 0.3 wt% O.[26]

A study of reused EB-PBF Ti-6Al-4V powder microstructure, crystallography, and nanohardness was carried out by Wei et al. in 2018 to address the changes in the powder due to the complex thermal histories of the particles from the EB-PBF process.[62] The authors carried out the study on an Arcam Q10plus EBM machine with plasma atomized powder received from Arcam. The build process included producing concave acetabulum cups using the same machine settings for all of the builds. The powder handling process began with 80 kg of virgin powder in the machine hoppers. The builds were carried out such that each build would approximately consume 10 kg of powder. After each build, 200 g of non-sintered powder was collected from the same location on the build table. The remaining 70 kg of powder was sieved and mixed with 10 kg of virgin powder, which then it was introduced back into the hoppers such that the leftover 70 kg was increased back to 80 kg for the next build (Process B). The O and N content was measured in accordance with ISO 22963:2008[58] whereas Al and V were measured in accordance with ASTM E2371-13.[56] Microstructural analysis of the virgin powder revealed primarily α and α′ phases. The authors note that after 1 reuse, the β phase became visible. Near-equiaxed prior β grains were observed after the 4th powder reuse, and after 5 reuses the authors observed the α phase boundaries disappear from the microstructure. After 6 reuses the microstructure transformed to lamellar α + β, followed by lamellar colonies and Widmänstatten structures after the 7th reuse. The X-ray diffraction analysis revealed a narrowing of the hexagonal peaks after reuse. The oxygen content of the virgin powder was measured to be 0.12 wt% O, which rose to 0.15 wt% O after 4 reuses, and remained stable at 0.15 wt% O up to 7 reuses. The authors concluded that with increased powder reuse, the non-equilibrium α′ converts to equilibrium α + β. The nanohardness and Young's modulus obtained from the nanoindentation experiment were observed to increase over powder reuse times, and tensile properties of the as-built bulk samples were similar to the parts fabricated from virgin powder.[62]

A 2018 study was conducted by Sun et al. in order to compare virgin Ti-6Al-4V powder feedstock differences in particle size distribution, microstructure, chemistry, surface morphology, flow characteristics, and packing density.[63] Two gas atomized Grade 5 Ti-6Al-4V from two different vendors and one plasma atomized Grade 5 powder sample from a third vendor were provided along with a Grade C powder provided by a 4th vendor (authors note that 'Grade C' is an outdated nomenclature, equivalent to Grade 5). Gas atomized Grade 23 Ti-6Al-4V powders were provided by an additional two vendors, bringing the total to 6 independent commercial vendors for the powder feedstock investigation. All of the powder examined in the study complied with the ASTM F2924-14 standard

for PBF AM processes.[35] There were noted differences in the particle size distribution, with smaller PSD visible in the Grade 23 powders. The plasma atomized Grade 5 Ti-6Al-4V powders were shown to exhibit the smoothest particle surface, while the remaining powders contained attached satellite particles. All of the powders were shown by XRD to have HCP crystal structure and SEM analysis revealed martensitic α' acicular microstructure

A complimentary powder reuse study of EB-PBF Ti-6Al-4V was also conducted by Sun et al. in 2018 with specific emphasis on the oxygen distribution as a function of powder microstructure and morphology.[64] The 30 builds for this experiment were conducted with an Arcam A2X machine using Grade 5 Ti-6Al-4V in order to compare and contrast the effects of reused powder with respect to how oxygen affects the Ti-6Al-4V powder on a microstructural level. Sun et al. used the Arcam PRS to recover the sintered powder, according to Process A, and noted that the powder was not traced to exact locations in the build chamber and therefore represented a mixture of sintered and surrounding powder from various builds. The powder bed was preheated to 600 °C with a partial vacuum of He $\sim 4 \times 10^{-3}$ mbar. The virgin and reused Ti-6Al-4V powder were characterized via a LECO ONH 836 machine in accordance with ASTM E1409-13,[55] X-ray diffraction, scanning electron, and scanning transmission electron microscopy. The authors noted that at low magnification, there were little to no visible morphological differences between the virgin and reused powders. However, at higher magnifications the surfaces of the reused powder were coarse, irregular, and exhibited 'crater-like' indentations; of which Sun et al. suggested might be a result from plastic deformation occurring during the powder reuse process. XRD analysis revealed sharper peaks for the α phase in the reused powder, indicated by the authors as a result of the elimination of crystal defects and coarsening of the α phase of the reused powder. The authors indicate that via use of the prescribed Arcam reuse procedure, the average oxygen concentration increases from 0.15 wt% to 0.205 wt% O. However, the oxygen increase is not a gradual accumulation of the oxide surface layer. It was observed that the martensitic α' microstructure of the virgin powder converts to an $\alpha + \beta$ microstructure, of which oxygen incorporates preferentially into the β phase.[65] The authors noted that the distribution of highly oxidized particles in a reused powder batch is substantially inhomogeneous, with significant local particle variations revealed in the microstructural analysis, which the authors suggest might potentially impact the fatigue behavior of AM produced parts. Sun et al. conclude that the reused powders ultimately have a narrower PSD and coarser morphology than virgin powder and that the microstructures of reused powder particles range from the metastable α' to equilibrium $\alpha + \beta$, with excess oxygen of the powder batches being accumulated in the β phase.[64]

A study by Popov et al. was carried out to investigate the effects of powder reuse on the microstructure and mechanical properties of as-built and HIPed Ti-6Al-4V samples (Fig. 5).[29] The aims of their experiments were to identify a reasonable number of powder reuses, what were the requirements for a successful reuse procedure, and what are effective post-processing procedures for good mechanical properties. The samples were additively manufactured using Grade 23 powder supplied by Arcam on an Arcam A2X machine. The melting was carried out under vacuum less than 1.5×10^{-4} mbar. The virgin powder oxygen concentration was measured to be 0.124 wt% O. Powder reuse was carried out in accordance with the recommended reuse procedure by Arcam (Process D). The concentration of oxygen increased to 0.132 wt% O after 11 reuses, 0.167 wt% O after 26 reuses, and 0.324 wt% O after 69 reuses. The mechanical and fatigue testing were conducted on the as-built and HIPed specimens built from the powder batch that was reused 69 times. Microstructural characterization revealed no apparent differences in the as-built and HIPed microstructures from virgin and reused powder. However, the authors noted that during mechanical testing, elongation and reduction in area of the material built from reused powder was significantly lower than in the material built from a virgin powder batch. The authors demonstrated that HIP improved the fatigue strength of the material even after 69 powder reuses but still not enough to qualify for aerospace standards. Note that these tests were done on a reused powder that contained 0.324 wt% O, which falls outside of the ASTM F2924-14 standard[35] for Grade 5 Ti-6Al-4V feedstock used in powder bed fusion. Therefore caution must be taken when inferring general trends in behavior of AM parts built from Ti-6Al-4V powder that has been reused, as the aforementioned studies have shown that there is an achievable limit of powder reuse that can still yield mechanical properties that fall within industry standards. A powder sintering study by Yan et al.[66] on as-sintered Ti-6Al-4V established that there exists a critical level of oxygen content ($\sim$ 0.33 wt% O) where ductility dramatically decreases when the concentration of oxygen is greater than 0.33 wt% O. Therefore, the reduction in ductility observed by Popov et al. is consistent with the observations made by Yan et al.[66]

Recently, work by Chandrasekar et al. concentrated on the effects of EB-PBF Ti-6Al-4V powder reuse as evaluated by the process log data in-situ.[67] The work by Chandrasekar et al. focused on a data-driven methodology to characterize the behavior of reused powder in-situ via analysis of log file data from the sensors in the AM machine. With the efforts of this study focused on reducing the amount of costly ex-situ analysis, the authors proposed

analyzing the rake motion during the build process to study the spreadability of the powder. The authors utilized the process log data collected from the earlier powder reuse experiments of Inconel 718 and Ti-6Al-4V by Nandwana et al. in 2016[59] which were carried out on an Arcam A2 EBM machine. For the Inconel 718 powder, it was discovered that powder reuse led to increased rake passes after the third build, of which the authors believe is due to the sintering kinetics causing powder agglomeration. Analysis of the Ti-6Al-4V build process log data showed virtually no correlation between re-raking and reuse times, which is in contrast to what was observed for the Inconel 718 powder. The authors attribute this difference in re-raking to the differences in sintering kinetics for each of the alloys, as it was calculated that the Ti-6Al-4V powder sinters twice as fast per layer than the Inconel 718 powders, leading to large Ti-6Al-4V particle agglomeration that subsequently gets sieved out during reuse process prior to the next build. Chandrasekar et al. also pointed out that the first build of the Ti-6Al-4V powder has significantly lower re-raking than subsequent builds, which they propose is attributable to oxidation during the build process and moisture pickup during the powder reuse steps.[67]

A study of the oxide surface of reused Ti-6Al-4V powder via X-ray photoelectron spectroscopy (XPS) was conducted by Cao et al. in order to characterize the surface morphology and oxide thickness resulting from powder reuse.[68] Commercial plasma atomized Ti-6Al-4V powder was used in an Arcam Q10plus system and was sieved and put back into the hoppers for subsequent use without the addition of virgin powder (Process A). The layer preheating conditions were approximately 600 ° C–750 ° C. The oxide thickness of the surface via XPS was measured to be 6.5 nm for the virgin powder, followed by 7.35 nm and 7.54 nm for the 5th and 10th reuses, respectively. Auger electron microscopy was used to investigate powder surface chemistry where the authors noted that Al-content was overall decreased due to Al evaporation. However, there were localized regions of the powder with Al-enrichment due to the high Al affinity for oxidation. The authors also stated that there were local variations in oxide thickness and chemistry on individual powder particles from the reuse process.[68]

Another study of EB-PBF Ti-6Al-4V by Shanbhag et al. in 2020 detailed the effects of powder reuse on particle size, flow, and rheometric properties.[69] The authors, using an Arcam A2X machine, compared four Grade 5 Ti-6Al-4V powder conditions consisting of virgin powder, powder that was reused once, twice, and an equally blended powder from the 1st and 2nd reuse batches. The reuse process consisted of using the Arcam PRS and a vacuum cleaner to retrieve unused powder from the AM chamber, followed by sieving with a mesh size of 105 μm and then reintroduction into the powder hoppers. Using the terminology introduced by Popov et al.,[29] the authors categorize 'clip-clap', broken, shattered, agglomerated, satellite, deformed, and elongated particle defects in the reused powder. The authors noted satellites present in the virgin powder, which were significantly less frequent after the first reuse. There was a narrower PSD after the 1st reuse which broadened again after the 2nd with a general decrease in particle sphericity. The authors noted a decrease in flowability, attributed to a reduction in spherical particles and the introduction of defects and irregularities from the reuse process.[69]

Three articles stemming from the same 30 builds of reused Ti-6Al-4V powder were recently published that detail the oxygen content and effects on mechanical properties of the built parts,[70] fractographic features of the parts built with the reused powder,[71] and the general powder morphology and part microstructure of EB-PBF Ti-6Al-4V built from the reused powder over the 30 builds.[72] The 30 builds consisted of Grade 5 Ti-6Al-4V used in an Arcam A2X EBM machine. The reuse process consisted of using the PRS to blast away the sintered powder, where it was then collected and mixed with the remaining powder in the hoppers before it was sieved and reintroduced into the hoppers for the next build. This is in contrast to the recommended Arcam powder reuse process, which calls for the introduction of virgin powder in between each build. As a control, virgin powder was put through the PRS system for 30 h to simulate the mechanical deformation of the powder from the process without varying the thermal history like the powders that are exposed to the beam inside the AM chamber. For each of the 30 builds, the authors developed standardized test specimen geometries for the builds that consisted of 40 cm^3 of metal that included 0.6 cm^3 of support metal. The total volume of the powder in the build chamber was noted by the authors to be 2966 cm^3 that was based on the total build height of 104 mm. The build chamber preheating was set to the default machine preheat temperature of 650 ° C. The build time for all 30 builds was 480 h. The machine settings included a beam speed of 4530 mms/s at a current setting of 15 mA (max current 20 mA). X-Ray fluorescence was used for chemical analysis of the Ti, Al, V, Fe, and Y whereas inert gas fusion using a LECO Model 836 was carried out for O, N, and H analysis. Ghods et al. noted decreased sphericity in powder morphology after four powder reuses, as well as an elimination of the smaller particles. The surface deformation of the powder particles increased as a function of reuse and irregular morphologies became more frequent such as appearance of fractured, fused, and recast particles with increased powder reuse. The authors describe small chemical changes in the V and Al content of the Grade 5 powder, such that V content change was observe to be negligible while the Al content rose by 0.03 wt% Al over the 30 builds. There was also a noted

increase in Fe content from 0.21 to 0.29 wt% Fe. The concentrations of H and N remained constant and within the limits for the ASTM F2924 standard.[35] Ghods et al. observed a linear increase in O content as a function of reuse times similarly to the previously described powder reuse studies. The initial oxygen concentration of the virgin powder was measured to be 0.142 wt% O, which crept up to 0.189 wt%, 0.269 wt%, and 0.356 wt% O after 10, 20, and 30 builds, respectively. The bimodal particle size distribution of the virgin powder transitioned to a Gaussian distribution with powder reuse.[72] With increasing reuse and powder oxidation, the as-built parts in both horizontal and vertical build directions saw increases in yield and ultimate tensile strengths while showing a decrease in elongation.[71] Fractography of the as-built parts from the Ghods et al. study revealed that failure occurred at the surface of all as-built specimens as well as microvoid coalescence in all of the fracture surfaces regardless of reuse times.[71] Schur et al. highlight that failure of the horizontal specimens occurred at the last printed surface, which they attribute to the likelihood of a finer surface microstructure of the surface. The appearance of fracture flutes were observed in all builds after the 12th build, which the authors attribute to a reduction in slip of the α phases due to the increased oxygen content with powder reuse.[71] An evaluation of the powder particles resulting from each of the reuse times revealed that the complex thermal histories present in the powder from the EB-PBF process results in increased coarsening of the powder as well as surface hardening due to contamination from oxidation and other sources. Mechanical deformation of the powder resulted in work hardening, however the Montelione et al. study suggest that this was not a significant factor in powder reuse other than that changes in powder morphology will affect flowability and spreadability of the powder during the EB-PBF process.[70]

Laser Powder Bed Fusion

Similar to the EB-PBF reusability studies, there were few studies pertaining to the reuse of Ti-6Al-4V powder for L-PBF only until recently. One of the first studies focusing on the reuse of Ti-6Al-4V powder used in L-PBF was a 2012 study conducted by Seyda et al. where the authors had suspected that, through reuse, changes in the Ti-6Al-4V powder were taking place similarly to what was being observed in steels.[73] The authors used commercially available gas atomized Ti-6Al-4V powder with particle size D90 (50 μm), but do not note whether Grade 5 or Grade 23. Their setup consisted of a 200-W fiber laser with 'standard exposure parameters' and layer thickness of 30 μm. The powder was used in 12 builds over several months, where the reuse procedure consisted of sieving with an 80- μm mesh and reintroduction back into the production cycle. As-built test specimens were built in cube shape for measurement of density, porosity, hardness, and surface finish, whereas tensile bars were built to study mechanical properties. The authors note that no post-processing was performed on the as-built samples. Seyda et al. observed that powder reuse leads to powder coarsening and increased flowability (qualitatively, by imaging heaps of powder) and particle size distribution, as well as increased density in the as-built parts when compared to those built with virgin powder.[73]

A 2015 study by O'Leary et al., a collaboration between Cardiff University and Renishaw, investigated the reuse of Ti-6Al-4V powder in order to establish a research methodology[74] for reused Ti-6Al-4V powder and to understand the relationship between reused powder and finished part properties. The aim of their work was to demonstrate that the process can produce Ti-6Al-4V parts via L-PBF that are up to industrial standards. The L-PBF process used 40 kg of virgin Grade 23 powder over 5 identical builds such that the entire batch would be consumed over the 5 builds. After the builds were complete, the remaining powder was swept into overflow containers for sieving before being introduced back into the feed regions. The processing conditions consisted of 200-W laser power for the volume area and borders with an exposure time of 65 μs and 35 μs, respectively. Through the reuse process, the authors observed an increase in PSD with a reduction of fine particles, as well as surface roughening and reduced sphericity. The LECO chemical analysis revealed the oxygen content of the virgin powder to be very close to the 0.13 wt% O Grade 23 limit, which fluctuated slightly across builds 2–4, finally resulting in the same 0.13 wt% O after the 5th build. Consequently, the oxygen content of the as-built part decreased steadily across the builds, initially being over the 0.20 wt% O limit of Grade 5 Ti-6Al-4V to being approximately 0.19 wt% O.[74]

A 2016 white paper by Renishaw details the effects of Grade 23 Ti-6Al-4V reuse on chemistry, flow, density, and PSD in their AM250 system over 38 builds.[75] The 38 builds of standard volume 250 mm × 250 mm × 300 mm were built with layer thicknesses of 20 μm to 100 μm with a 200-W laser. The chamber was purged and back-filled with Ar in a process that required 600 L of Ar. The builds were carried out with the same reused powder without the introduction of any virgin powder, so that the powder was mostly consumed throughout all the builds. The reuse process consisted of introducing powder into the chamber feed region. Then, recovered powder from the powder-bed was collected into overflow bottles retaining the inert Ar atmosphere of the chamber, sieved, and reintroduced into the top of the feed region without coming into contact with air. The reused powder sampling was carried out in situ by means of printing a hollow powder capture capsule during the build process, which was

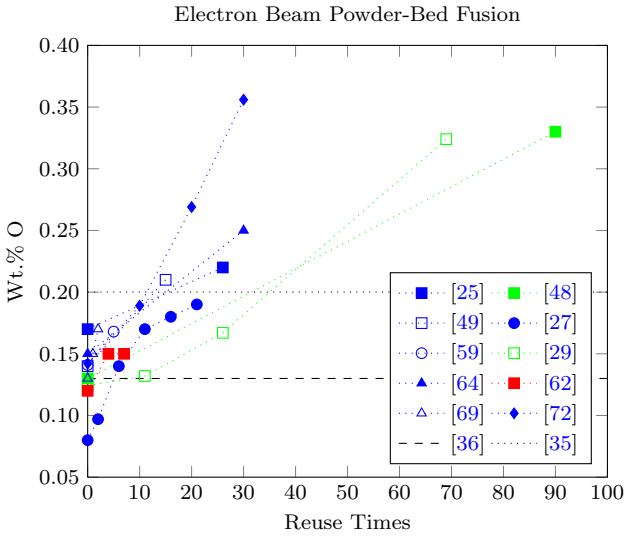

Fig. 6. Oxidation rates from the Ti-6Al-4V powder reuse studies related to EB-PBF AM. Plot colors of blue, red, and green pertain to Process A, Process B, and Process D, respectively (Color figure online).

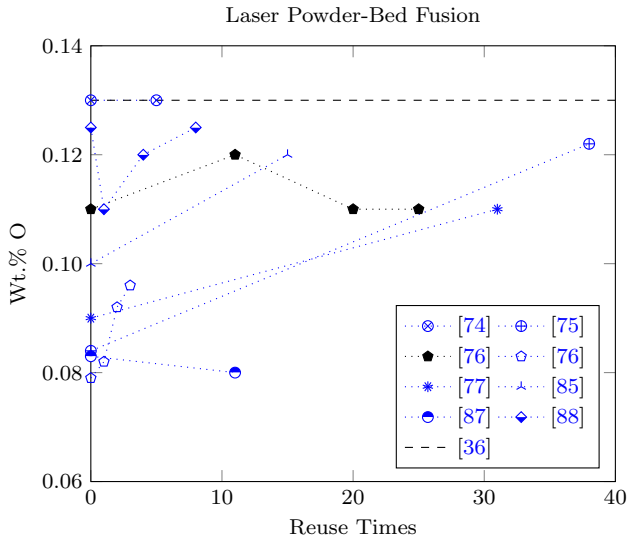

Fig. 7. Oxidation rates from the Ti-6Al-4V powder reuse studies related to EB-PBF AM. Plot colors of blue and black pertain to Process A and Process C, respectively (Color figure online).

then closed off as the build reached an appropriate height which was designed to be the same height as the tensile bars that were built. The PSD was measured via wet laser diffraction to obtain the D10, D50, and D90 values of the powder, which stayed relatively the same over the 38 builds, with a small narrowing of the PSD over the builds. The Hall flow speed increased due to powder reuse, which was correlated with the slight increase in D50 values; however, it was noted that this did not significantly affect build parameters or layer spreading. Oxygen increased to the upper Grade 23 limit of 0.13 wt% O after 16 builds, and fluctuated slightly above and below this limit for the remaining builds, up to 38. Nitrogen content also increased throughout the powder reuse, but at a much slower rate to 0.03 wt% after 36 reuses. Tensile specimens were tested across the builds, with an increase of 100 MPa in UTS from virgin to the 38th powder reuse, attributed to the increase in oxygen and nitrogen content. The UTS of the machined specimens compared to the as-built specimens were also approximately 100 MPa higher, which the author suggests could be effects from the rough surface finish of the as-built samples leading to more crack initiation sites or from error in the cross-sectional measurement due to the rough surface finish.[75]

A 2017 study by Thejane et al. investigated the effects of Grade 23 Ti-6Al-4V powder reuse on two different L-PBF machines.[76] The experiments consisted of 25 powder reuses on a direct metal laser sintering (DMLS) system and 10 reuses on a concept laser system. The powder used in the DMLS machine showed poor flowability, so was first dried at 80 ° C for 5 h, followed by sieving prior to the first build. The powder was then reused 10 times, after which there was no longer any powder left to complete further builds. Virgin powder was then added on the 11th build onward to the 25th. The reuse process for the concept laser system involved 10 builds without any introduction of virgin powder into Process A. Thejane et al. observed that less oxygen pickup occurs during the room-temperature operation of the L-PBF systems when compared to the elevated temperatures of an EB-PBF machine.

A study of tensile and fatigue performance for gas-atomized Grade 5 and Grade 23 L-PBF Ti-6Al-4V was conducted by Quintana et al. in order to isolate the effect of oxygen concentration from the difference in Ti-grades on the mechanical properties.[28] The authors manufactured 46 bars from both Grade 5 and Grade 23 powder types (measured to contain 0.16 wt% O, and 0.11 wt% O, respectively) and applied HIP treatment at 920 ° C at 102 MPa for 2 h to 36 of the samples. Several of the HIPed samples were used for microstructural characterization while others were used for rotating beam fatigue testing in both smooth and notched conditions. The oxygen content was measured via inert gas fusion for the as-built and HIPed bars built from both grades of Ti-6Al-4V powder. The bars built via Grade 5 powder were measured to contain 0.162 wt% O and 0.164 wt% O, respectively. The O content of the as-built and HIPed bars made from Grade 23 powder was measured to be 0.118 wt% O and 0.110 wt% O, respectively. Quintana et al. reported that the bars built via Grade 5 Ti-6Al-4V powder displayed greater YS and UTS in both the as-built and HIPed conditions than the Grade 23 Ti-6Al-4V powder, with Grade 5 specimens also showing greater elongation in the HIPed condition than the Grade 23 parts. However, opposite elongation

effects were observed in the as-built conditions, such that the Grade 23 Ti-6Al-v showed greater elongation than the Grade 5 specimens. The fatigue life endurance of the HIPed specimens from Grade 5 powder was 50 MPa greater than that of those built via the Grade 23 powder, correlated with the higher tensile strength of the Grade 5 part. There were no noted differences in fatigue endurance limit in the notched condition for the HIPed bars made from both grades of Ti-6Al-4V powder.[28]

A follow-up study by Quintana et al. investigated the effects of Grade 23 Ti-6Al-4V powder reuse on the built part chemistry and mechanical properties.[77] The authors used 100 kg of gas-atomized Grade 23 Ti-6Al-4V. The reuse process consisted of transferring the powder from the build plate into an overflow container to be sieved and reintroduced into the feed regions without the addition of any virgin powder. The sampling process differed slightly from the previous studies in that powder sampling was conducted both before the build and in situ with the use of trap capsules. The authors carried out 31 builds, taking 'before' samples at 10 dispersed times throughout (after they had been sieved from the previous build), to correlate with the powder collected via the trap capsules. These powder samples were collected on the 4th, 6th, 8th, 11th, 15th, 17th, 19th, 23th, 27th, and 31st builds. Two additional trap capsule samplings were carried out during the 1st and 5th builds. Tensile tests were carried out on HIPed samples from the 1st, 4th, 17th, and 31st builds. Oxygen/nitrogen contents were measured in accordance with ASTM E1409,[55] Al/V content, as per ASTM E2371-13.[56]. Particle size distribution, flowability, and tap density were measured in accordance with ASTM B822-17,[78] ASTM B213-17,[79] and ASTM B527-15,[80] respectively, the latter two having since been superseded by ASTM B213-20[81] and ASTM B527-20.[82] Tensile testing of the HIPed specimens was in accordance with ASTM E8/E8M-16a.[83] The trap capsules saw an increase from 0.09 wt% O to the Grade 23 limit of 0.13 wt% O after 31 builds, whereas the samples collected before the builds saw an increase of 0.09 wt% O to 0.11 wt% O. The authors noted that there was generally more oxide present in the powder collected via the trap capsules, likely due to the proximity to the melt pool, whereas the 'before' powder samples were collected from sieved powder once the L-PBF process had been completed. The authors recorded no noticeable difference in Al/V contents from the reused powder to the as-built and HIPed specimens. The authors noted that the powder PSD measured via the D85 value saw a decrease after powder reuse, while the morphology slowly shifted towards fewer satellites and coarser particles after 31 builds. There was an improvement in flowability with a small decline in tap density with increased powder reuse. The authors observed slight increases in YS and UTS after the 31 builds due to oxygen strengthening but no noticeable effects on ductility.[77]

The effects of powder reuse on fatigue behavior in L-PBF Ti-6Al-4V was carried out by Carrion et al., where mechanical properties of parts built from virgin powder were compared those built from powder that had been reused 15 times.[84,85] Test specimens were fabricated with an EOS M290 L-PBF system using gas-atomized Grade 23 Ti-6Al-4V powder, with the PSD ranging from 15 to 45 μm. Machine parameters included a 280-W laser, 1200 mm/s scan speed, 100 mm stripe width, 140 μm hatch spacing, and 30 μm layer thickness. The reused powder was first sieved with an 80- μm mesh before reintroduction into the feed regions. Oxygen and nitrogen were measured using a LECO ONH-836, in accordance with ASTM E1409-13.[55] Two material conditions were tested, as-built cylinders (net shape) and rectangular bars that were machined. All the test specimens were annealed at 704 ° C for 1 h in Ar for stress relief prior to testing. The authors record an increase from 0.10 wt% O to 0.12 wt% O after 15 reuses, which showed negligible effects on the microstructure of the as-built material. As the PSD became narrower, the flowability of the powder increased. There were negligible effects on tensile strength and fatigue behavior for both virgin and reused conditions in the as-built condition. Samples with machined surfaces had noticeable difference in the high cycle regime, such that the material built from reused powder had longer fatigue lives.[85]

In an effort to achieve "more consistent and economical reycling of raw materials for PBF processing", Denti et al. proposed a new 'average usage time' (AUT) parameter that incorporates usage time of the powder as well as virgin-to-used powder mixing ratio during L-PBF of Ti-6Al-4V alloy.[86] The aim of this parameter is to incorporate the different types of jobs that require different build times as a function of geometric shape, as well as the varying levels of virgin powder added to the batch for a subsequent build. For the experiments, the reuse procedure consisted of initially filling the powder feed region to capacity. At the end of each build, all of the powder was mixed and sieved with an 80-μm mesh in inert gas. If the reused powder was determined to be appropriate in volume for the next build, then no virgin powder was added. If there was an insufficient amount of powder to complete the following build, then virgin powder was added. For the experiment, the powder reuse process was carried out 100 times, which corresponds to an AUT of 1750 h (the details of the calculation that combines job time with a modified rule of mixtures can be found in Ref. 86). The machine parameters for the builds followed standard process parameters for the EOS M290 machine (laserpower = 280 W; Scanspeed = 1200 mm/s; layer thickness 30 μm; hatchspacing = 140 μm.) The authors did not observe any increased oxidation on the finished parts, which may have been due to continual additions of virgin powder to the reused powder.

Similar to the previous studies, a narrower PSD led to better flowability of the powder. The authors concluded that YS and UTS remained stable throughout the reuse process up to an AUT of 1750 h.[86]

The effect of powder reuse on gas-atomized Inconel 718, Scalmalloy (Al, Mg, Sc), Al-Si-10Mg, and Ti-6Al-4V powders were characterized in order to determine the effects of the reuse procedures on these four specific powders.[87] The experiments were carried out on an SLM Solutions 280. The Ti-6Al-4V was reused 11 times without the addition of any virgin powder. The oxygen content was measured both by LECO and EDX, with LECO values showing slight decreases in oxygen concentration due to reuse for Ti-6Al-4V. The Ti-6Al-4V PSD remained relatively stable in size with increased flowability. The authors conclude their study detailing a flow chart for the feasibility of powder reusability.[87]

A recent study by Alamos et al. investigated the mechanical response as affected by powder reuse paired with process optimization of build parameters using a factorial design of experiments.[88] The powder was cycled through eight builds, and was recovered and sieved with a 63-μm mesh. There was no blending of reused and virgin powders. The authors concluded that no noticeable changes in mechanical properties were observed after the eight reuses other than a small increase in oxygen content in the as-built material (0.125 wt% O → 0.140 wt.% O).[88]

DISCUSSION AND SUMMARY

Thermodynamics and Oxidation Kinetics of Ti

This section briefly discusses the current understanding of titanium oxidation thermodynamics and kinetics, which will provide specific scientific context to the following sections assessing the potential for oxidation rate across multiple AM builds to be affected by variations in the powder reuse methods.

Titanium alloys will form a stable oxide layer at room temperature and are notoriously prone to faster rates of oxidation at higher temperatures. Therefore, processing Ti requires a highly inert gaseous environment to maintain purity, namely free of oxygen contaminants. An Ellingham diagram, adapted from Ref. 89, is presented in Fig. 8 to highlight the partial oxygen pressures for equilibrium oxide production for Al, Ti, and V. In short, Al reduces Ti, which reduces V. The free energy for Al_2O_3 production is lower than that for TiO_2 production. However, in Ti-6Al-4V, the majority of the total oxidation that occurs is due to the presence of Ti, simply because of the larger mass fraction of Ti to Al in Ti-6Al-4V. Metallurgical processes with reactive metals will often employ gas purification that utilizes Ti as a gettering media to scrub the cover gas of impurities.[90–93] For example, the equilibrium partial pressure of O_2 for the $Ti + O_2 = TiO_2$ reaction at the melting point of Ti is $\approx 10^{-16}$ atm ($\sim 10^{-13}$ mbar). Therefore, any partial pressure of $O_2 > 10^{-16}$ atm will cause Ti to oxidize and form TiO_2. Partial pressures of $O_2 < 10^{-16}$ will lead to TiO_2 decomposition into pure Ti and O_2 at the melting temperature of Ti. At temperatures higher than the melting point of Ti, which is often the case with PBF processes, the melting and boiling points of TiO_2 (1843 °C and 2972 °C, respectively) may be surpassed. These temperatures have the potential to result in liquid TiO_2 slag that may be pushed around and/or away from the melt pool, potentially to regions of unmelted powder and should be taken into consideration when critically assessing powder reuse.

Early high-temperature oxidation studies of Ti demonstrated that oxidation at pressures above $\sim 10^{-3}$ mbar and below 1300 °C mainly produced rutile, TiO_2, while pressures lower than 10^{-3} mbar and higher than 1300 °C saw the production of Ti_2O, TiO, Ti_2O_3, and Ti_3O_5 as well as TiO_2.[94] Recent studies of the oxidation kinetics in commercially pure Ti in air demonstrate that the anatase form of TiO_2 was produced on the surface from 276 – 457 °C, with mixed anatase and rutile phases up to 718 °C, followed by only rutile TiO_2 above 718 °C.[95] The oxidation of Ti at high temperatures is measured to be generally parabolic,[96–98] consisting of two contributing factors: formation of the rutile TiO_2 scale and oxygen diffusion into the bulk α-Ti. Comparative studies of Ti and Ti-6Al-4V in gaseous water vapor environments showed similar parabolic oxidation rates for both Ti and Ti-6Al-4V.[99] The activation energy of oxidation of Ti-6Al-4V is also comparable to pure Ti.[100] Motte et al. pointed out, however, that oxidation in H_2O vs. O_2 are fundamentally different, such that the kinetic curves from the oxidation in pure O_2 showed many stages rather than the parabolic behavior seen in H_2O gas over

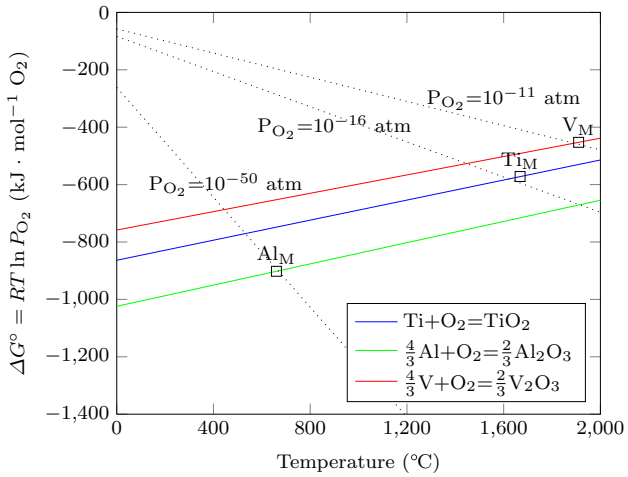

Fig. 8. Ellingham diagram for Ti, Al, and V. Adapted from Ref. 89.

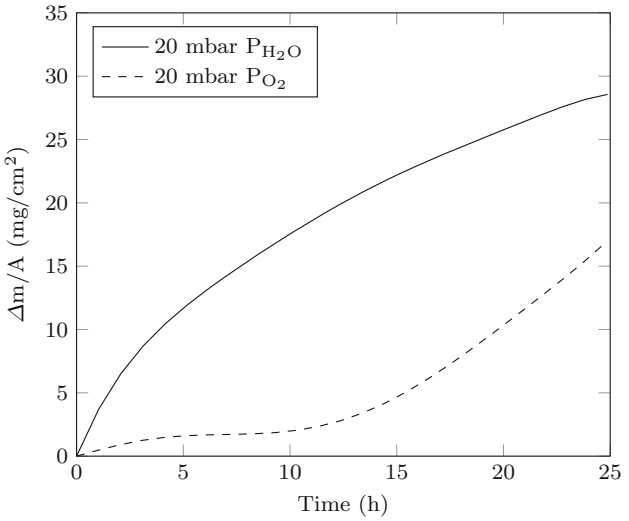

Fig. 9. Comparative oxidation kinetics of Ti at 850 ° C in 20 mbar O_2 and H_2O. Digitized and replotted from Ref. 101.

the same temperature ranges. Wouters et al. suggested that, in an H_2O environment, oxidation preferentially takes place via substitutional hydroxide ion transport through the TiO_2 surface scale. This thereby leads to higher oxidation rates in a water vapor environment as opposed to pure O_2, which is shown in Fig. 9, where the oxidation rate plot has been digitized and adapted from Ref. 101. These results indicate not only O_2 but also H_2O partial pressures contribute significantly to the oxidation of titanium. This understanding is important as both of these forms of oxygen may be contributing to PBF titanium powder oxidation, as discussed in section Additive Manufacturing of Titanium

Powder Oxidation and Chemistry Changes

The oxidation rates observed for both EB-PBF and L-PBF are drawn to the same scale in Fig. 10, in which the oxidation plots appear to show no direct correlations between the reuse methods used and powder oxygen content increase. This could be due to a number of reasons, and differences in each experiment, such as build volume, preheat/background/local temperatures, beam exposure time, and differences in powder reuse methods, at a level of detail not commonly reported in the literature. Thus, the authors recommend researchers report the following details in their powder reuse studies to enable a greater understanding of the oxidation and oxidation rates that occur in PBF Ti-6Al-4V:

- Virgin powder batch details: e.g., powder manufacturing type (plasma atomized vs. gas atomized), particle morphology (spherical vs. irregular), average particle size, powder size distribution, virgin powder full chemistry and comparison to pertinent material specification
- PBF process details: e.g., machine manufacturer/model, software version, melt parameters, layer thickness
- Preheat/background/local temperatures
- Type of inert gas used, bottle purity, and flow rates
- Heat-up/beam-on/cool-down times
- Relative humidity in the laboratory environment
- Total build volume/total mass of solid parts/total surface area of solid parts
- Mass of unmelted powder in build area, mass of powder remaining in hoppers/feed regions, and mass of virgin powder added after each build
- Powder characterization technique details, including any standards followed
- Powder sampling procedure: When during the process were powder samples taken? Where

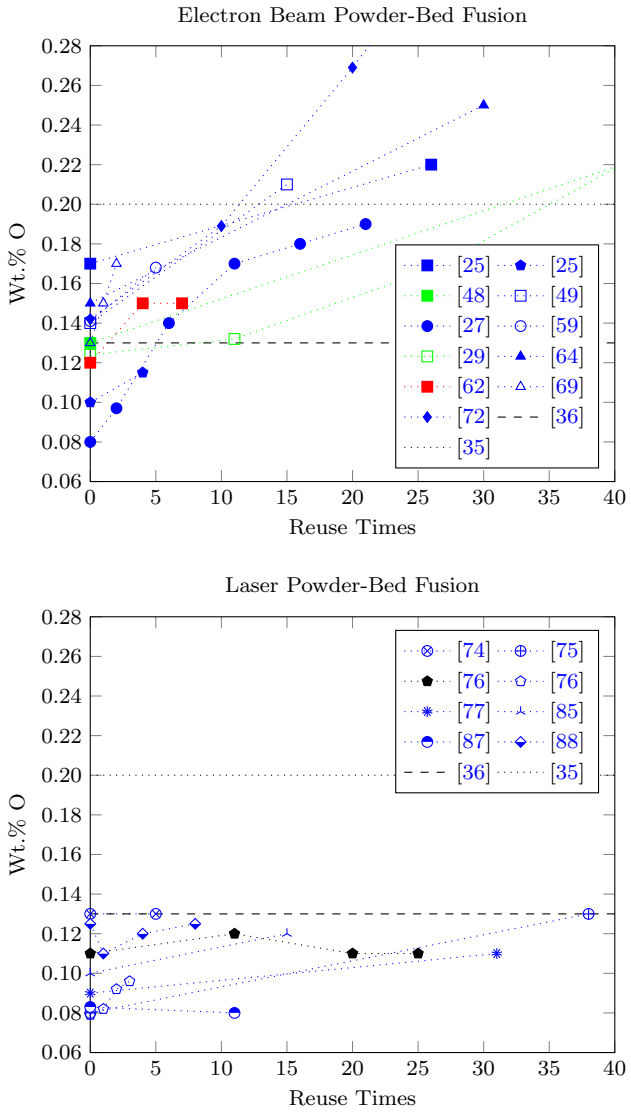

Fig. 10. Oxidation pick-up rates from the Ti-6Al-4V powder reuse studies related to both EB-PBF and L-PBF, adjusted to show equal axes. Plot colors of blue, red, black, and green pertain to Process A, Process B, Process C, and Process D, respectively (Color figure online).

exactly were powder samples taken? What mass of powder was taken/tested for each sample? What equipment was used to take samples and ensure they are representative of the entire batch of powder (e.g., riffler, thief)? If any standard sampling methods were used? If the standard leaves room for variation it is important to provide more detail as to the specific protocol used. If sampled from the powder bed, where and how it was sampled. There is a potential for significant changes in powder characteristics depending on proximity to melted parts.[102]

- Powder reuse method - Was virgin powder ever added to non-virgin powder? If yes, with what frequency and mass was virgin powder added? Was powder from the build area, virgin, and hopper/feed region powder ever mixed? If yes, how frequently did this mixing occur, what mixing technique was used (e.g., by hand, mixing by sieving, drum mixer with paddle inserts, v-mixer), and how long was mixing performed (including any mixing machine settings)?

From Fig. 10, it is clear that the high processing background temperature for EB-PBF of Ti-6Al-4V leads to a faster oxidation rate of the powder, as EB-PBF oxidation rates appear higher compared to L-PBF rates overall. This does not come as a surprise, as the temperature and pressures for TiO_2 production from the Ellingham diagram in Fig. 8 demonstrate that the preheat temperatures used in EB-PBF are in a range for TiO_2 production with very minimal oxygen partial pressure needed. This does not indicate that one process is better than the other, but rather that, when a high background temperature is used, there will be a greater likelihood for reactive metal powders to oxidize. For example, the Svensson study from 2009 showed drastic swings in oxidation of the powder that was sintered compared to the much smoother oxidation measurements from the mixed powder from all sources.[25] This illustrates a greater need for more accurate reporting moving forward in order to systematically characterize oxidation rates of Ti-6Al-4V feedstock.

The observation by Tang et al.[27] that Al content decreases significantly in powder over multiple reuses (6.35 to 5.93 wt% over 21 reuses) has important implications and will be discussed further despite being outside the scope of this review focused on oxidation effects. It is well known that Al selectively vaporizes during EB-PBF due to the vacuum environment and high background temperature of the process, as well as the relatively low vaporization pressure of Al. To ensure as-built EB-PBF material conforms to material specifications (6.75–5.5 wt%[35]), powder manufacturers produce Ti-6Al-4V powder intended for EB-PBF to have Al content on the high end of the allowable Al content range to accommodate the loss of Al during melting in the EB-PBF process. The observations from Tang et al. suggest that Al is also vaporizing from unmelted powder in the build area that will be resused in later builds. This phenomenon of Al loss in powder over multiple reuses is not well known, and may lead to Al content in as-built EB-PBF falling below material specification allowable limits after a certain number of powder reuses. It seems that further investigation of this phenomenon is warranted and may lead to factors other than oxygen content dictating the end of the usable life of a given EB-PBF Ti-6Al-4V batch of powder.

Nitrogen content also changes during the PBF process, as observed by the 2016 white paper by Renishaw,[75] suggesting that more work is required to understand the dynamics and rate of this change in the context of material specification limits. Nitrogen content was seen to increase in reused powder, eventually reaching material specification limits. Renishaw noted that it took more reuses for nitrogen to reach allowable limits compared to oxygen, which suggests that they feel that oxygen is still the limiting element when considering the usable lifetime of a powder batch. However, they only considered the Grade 23 limit for oxygen (0.13 wt%[36]). Since the Grade 5 limit for oxygen is much higher than Grade 23 (0.20 wt%[35]), and the nitrogen limit does not change for Grades 5 and 23 (0.05 wt%[35,36]), it seems that further investigation is necessary before concluding that nitrogen is not the limiting element in determining the usable lifetime of EB-PBF Ti-6Al-4V batches of powder.

Ultimately, these powder reuse studies raise the question of how accurate is the rule of mixtures when assessing Ti-6Al-4V powder batches for oxygen content; that is, could it be that small heterogeneous portions of powder batches play a larger role in material properties of AM parts? Studies across all types of powder reuse processes displayed nonlinear oxidation rates (Fig. 10[27,29,62,76,88]), and this may indicate oxygen content heterogeneity within a batch of powder that arises from insufficient mixing, over many builds, of powder batch subsets (i.e., virgin, build area, and hopper/feed region powder) with dissimilar oxygen content. Even Process D, which does not include any mixing of build area and hopper/feed region powder, displays nonlinear oxidation rates (Fig. 10[29]), possibly indicating oxidation within a given build area is heterogeneous. This could be in part due to insufficient mixing, given that reused powder batches tend to be very similar in morphology and flow characteristics save for differences in oxygen content. The combination of both virgin and reused powder batches, whether in the form of reused powder being refreshed with virgin powder or the mixing of two or more reused batches, may constitute a combination of both traditional blending and random mixing. If the particle characteristics are similar, the mixing may come down to the laws of probability as opposed to some of the traditional

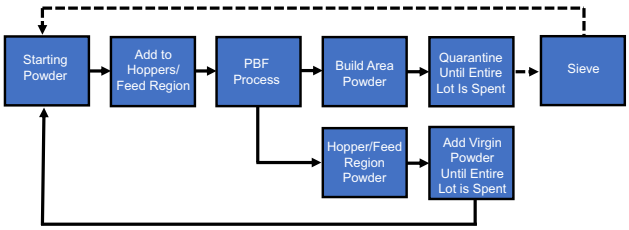

Fig. 11. Proposed powder reuse flow to mitigate heterogeneous oxygen concentration in powder batches.

driving forces that are present when mixing powder batches of different particle characteristics.[103] There is also a potential for varying oxidation rates as a function of powder size distribution, and this remains an open area of study for AM Ti-6Al-4V.

More information and studies are needed to elucidate the effects of high-oxygen-containing particles when mixed into powder batches with an overall low oxygen content. Although these mixtures may fall within the ASTM F3001 and F2924 standards for Ti-6Al-4V powder, the chemical extrema pertaining to the high-oxygen-containing particles may have the potential to negatively contribute to material performance, especially in AM components where a high degree of precision and geometrical complexity are required.

Potential Ways to Reduce Oxidation

Alternative Powder Reuse Flow

In order to potentially reduce the effects of oxygen heterogeneity in powder batches resulting from the powder reuse processes, one such process flow inspired by a combination of those in the literature is presented in Fig. 11. This process is very similar to those previously described; however, this powder reuse flow would quarantine all the build area powder (overflow, build plate, and sintered powder in the case of EB-PBF) for each individual build with no reuse. The entire starting lot of powder is consumed until the entire lot has gone through the machine once. This would ensure that a similar level of oxidation has occurred in the entire powder lot. This powder would then be blended and sieved prior to reintroduction into the process flow, thereby becoming the new starting powder batch. This method would reduce the highs and lows when it comes to particles containing oxygen as a function of the reuse process and smooth out the heterogeneous extrema in oxidation across the entire powder batch.

This proposed process flow may differ from what is already in practice for many research, governmental, or industrial production environments, and/or may already be in practice in some instances. The authors make no claims to whether this proposed powder reuse flow is better or worse for oxidation prevention. However, if the quarantining of the build area powder is only blended/mixed with

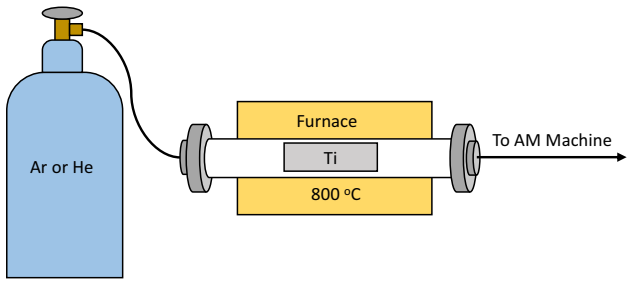

Fig. 12. Schematic demonstrating one example of a Ti-gettering gas purification setup.

powder that has been through the AM process the same number of times, it is the opinion of the authors that a more uniform oxygen distribution will be present in the entire lot. The idea being that less heterogeneity in the powder batches will positively affect the uniformity of mechanical properties across a single build.

Inert Gas Purification

Processing Ti at elevated temperatures is an atmospherically sensitive process owing to its high reactivity with and gettering of O_2, H_2, CO_2 and N_2.[90] Traditional melting and sintering of Ti at high temperatures is carried out under inert gas environments such as Ar and, less commonly, He. However, due to the extremely small partial pressures of oxygen for equilibrium formation of TiO_2, bottle purity of these gasses tends to not be enough for a high degree of purity when processing Ti alloys. Heated Ti has been traditionally utilized to reduce partial pressures of residual gasses in vacuum environments,[91] and is used to purify inert gasses by flowing the gas over Ti at 800 °C.[92] There exist several commercial gas purification furnaces that make use of these fairly straightforward processes for purification of inert gasses for high-temperature processing of reactive metals; however, the principles are simple enough for individual research groups/commercial AM part producers to build their own, as shown pictorially in Fig. 12.

For a Ti-gettering gas purification system as pictured in Fig. 12, the operating principles are that airtight fittings connect an inert gas cylinder such as Ar or He to an apparatus, typically a high-temperature tube furnace with Ti chips or a porous chunk of Ti placed near the heating element, heated to 800 °C. The gas flows over or through the Ti gettering media and exits via airtight connections to the AM machine. This Ti-gettering device can be easily implemented into an existing AM process, such that no machine settings need to be altered for the implementation of in situ gas purification, as it can be treated as an ultrahigh-purity gas instead of bottle purity. Through in situ inert cover gas purification for AM processes, specifically those that use reactive metals like Ti-6Al-4V, any oxygen and other impurities that may be contributed from the

cover gasses themselves can be removed. This is only one piece of the puzzle, however, as moisture in the powder/machine also contributes significant amounts of oxygen.

There have also been studies that make use of rare-earth elements such as cerium-based ($CeSi_2$)[104] and yttrium-based (YH_2)[105] compounds for oxygen scavenging in commercially pure Ti as well as Ti-6Al-4V. As these approaches introduce elements (Ce, Y) that may not be suitable for Ti-6Al-4V fracture-critical applications, they may be suitable for less demanding applications where internal chemistry may not need to be as rigorously controlled.

Summary

The oxidation of Ti-6Al-4V feedstock powder during powder-bed fusion (PBF) additive manufacturing (AM) is attributable to a number of potential factors: powder handling, background temperature, proximity to melted parts, exposure to atmosphere, humidity, and build chamber atmospheres. In order to extend the lifetime of powder batches and minimize the overall AM process cost, a critical understanding of key factors influencing oxidation and oxidation rate is needed. Titanium alloys, namely Ti-6Al-4V, are widely used in aerospace and medical industries for their high strength-to-weight ratios and good corrosion resistance. However, the high affinity for oxidation often leads to costly processing environments to maintain the purity of the finished product. Titanium feedstock powder needs to be handled with great care to ensure minimal oxygen contamination. Given that the lifetime of Ti-6Al-4V powder batches in a PBF production environment is often determined based on individual manufacturers' process optimization with respect to limiting oxidation in the Ti-6Al-4V powder, more information about powder reuse methods needs to be reported in the literature to accurately determine oxidation rates on a per-process basis. Findings and observations from the literature with respect to Ti-6Al-4V powder reuse across both laser (L-PBF) and electron (EB-PBF) powder bed fusion studies, as well as subsequent effects on material properties, have been summarized in this review. Note that the powder reuse methods described are not wholly representative of all powder reuse methodologies that exist throughout academic, government, and private institutions, but have been limited to those reported in the available literature.

The oxidation rates gathered from the literature were higher for EB-PBF compared to L-PBF, which is thermodynamically to be expected due to the the higher background temperature (400–800 °C) due to layer preheating in the EB-PBF techniques. There were no correlations between oxidation rate and powder reuse method, as significant variation in oxidation rate was observed within each powder reuse method employed in the studies. The authors feel that these results highlight a need for better reporting of powder reuse method details to appropriately assess the potential for the reuse method to affect the oxidation rate. Recommendations for powder reuse, gas purification, and details for more comprehensive powder reuse reporting are provided.

ACKNOWLEDGEMENTS

The authors wish to thank Jake Benzing, Ed Garboczi, and Justin Whiting for their helpful comments and discussions. This research was performed while N. Derimow held a National Research Council Postdoctoral Research Associateship at the National Institute of Standards and Technology (NIST).

CONFLICT OF INTEREST

The authors declare that they have no conflict of interest.

REFERENCES

1. N. Hrabe, N. Barbosa, S. Daniewicz, and N. Shamsaei, *NIST Adv. Manuf. Ser.* (2016). https://doi.org/10.6028/NIST.AMS.100-4.
2. T.T. Wohlers, I. Campbell, O. Diegel, R. Huff, and J. Kowen, *Wohlers Report* (Fort Collins: Wohlers Associates, 2019), pp. 1–369.
3. A. Totin, E. Macdonald, B. Conner, *DSIAC J.,* 6(2), 201 (2019).
4. D. Coney, M. Lasker, Aerospace Structural Metals Handbook. Code 3801 (1969).
5. ASTM F1472-14, *ASTM Standards* (2014). https://doi.org/10.1520/F1472-14.2.
6. M. Seifi, M. Gorelik, J. Waller, N. Hrabe, N. Shamsaei, S. Daniewicz, and J.J. Lewandowski, *JOM*, 69(3), 439 (2017). https://doi.org/10.1007/s11837-017-2265-2.
7. J.J. Lewandowski and M. Seifi, *Annu. Rev. Mater. Res.*, 46(1), 151 (2016). https://doi.org/10.1146/annurev-matsci-070115-032024.
8. S. Vock, B. Klöden, A. Kirchner, T. Weißgärber, and B. Kieback, *Progress Addi. Manuf.*, 4(4), 383 (2019). https://doi.org/10.1007/s40964-019-00078-6.
9. T. DebRoy, H.L. Wei, J.S. Zuback, T. Mukherjee, J.W. Elmer, J.O. Milewski, A.M. Beese, A. Wilson-Heid, A. De, and W. Zhang, *Progress Mater. Sci.*, 92, 112 (2018). https://doi.org/10.1016/j.pmatsci.2017.10.001.
10. D. Powell, A. Rennie, L. Geekie, and N. Burns, *J. Cleaner Product.*, (2020). https://doi.org/10.1016/j.jclepro.2020.122077.
11. N. Li, S. Huang, G. Zhang, R. Qin, W. Liu, H. Xiong, G. Shi, and J. Blackburn, *J. Mater. Sci. Technol.*, 35(2), 242 (2019). https://doi.org/10.1016/j.jmst.2018.09.002.
12. Z. Snow, R. Martukanitz, and S. Joshi, *Addit. Manuf.*, 28(2018), 78 (2019). https://doi.org/10.1016/j.addma.2019.04.017.
13. Z.Z. Fang, J.D. Paramore, P. Sun, K.S. Chandran, Y. Zhang, Y. Xia, F. Cao, M. Koopman, and M. Free, *Int. Mater. Rev.*, 63(7), 407 (2018). https://doi.org/10.1080/09506608.2017.1366003.
14. P. Kumar, K.S. Chandran, *Metall. Mater. Trans. A*, 48(5), 2301–2319 (2017). https://doi.org/10.1007/s11661-017-4009-x.
15. H. Conrad, *Progress Mater. Sci.*, 26(2–4), 123 (1981). https://doi.org/10.1016/0079-6425(81)90001-3.
16. P. Sun, Z.Z. Fang, Y. Zhang, and Y. Xia, *JOM*, 69(10), 1853 (2017). https://doi.org/10.1007/s11837-017-2513-5.

17. F. Cao, T. Zhang, M.A. Ryder, and D.A. Lados, *JOM*, 70(3), 349 (2018). https://doi.org/10.1007/s11837-017-2728-5.
18. A.H. Chern, P. Nandwana, T. Yuan, M.M. Kirka, R.R. Dehoff, P.K. Liaw, and C.E. Duty, *Int. J. Fatigue*, 119(2018), 173 (2019). https://doi.org/10.1016/j.ijfatigue.2018.09.022.
19. A.M. Beese and B.E. Carroll, *JOM*, 68(3), 724 (2016). https://doi.org/10.1007/s11837-015-1759-z.
20. J. Li, X. Zhou, M. Brochu, N. Provatas, and Y.F. Zhao, *Addit. Manuf.*, 31(2019), 100989 (2020). https://doi.org/10.1016/j.addma.2019.100989.
21. P.N. Sibisi, A.P. Popoola, N.K. Arthur, and S.L. Pityana, *Int. J. Adv. Manuf. Technol.*, 107(3–4), 1163 (2020). https://doi.org/10.1007/s00170-019-04851-3.
22. S. Liu and Y.C. Shin, *Mater. Des.*, (2019). https://doi.org/10.1016/j.matdes.2018.107552.
23. S.D. Luo, T. Song, S.L. Lu, B. Liu, J. Tian, and M. Qian, *J. Alloys Comp.*, (2020). https://doi.org/10.1016/j.jallcom.2020.155526.
24. M. Yan, W. Xu, M. Dargusch, H. Tang, M. Brandt, and M. Qian, *Powder Metall.*, 57(4), 251 (2014).
25. M. Svensson, Material Properties of EBM-Manufactured Ti-6Al-4V & Ti-6Al-4V ELI Under Raw and HIP Conditions. Arcam AB Internal Report, pp. 1–47 (2009).
26. W.A. Grell, E. Solis-Ramos, E. Clark, E. Lucon, E.J. Garboczi, P.K. Predecki, Z. Loftus, and M. Kumosa, *Addit. Manuf.*, 17, 123 (2017). https://doi.org/10.1016/j.addma.2017.08.002.
27. H.P. Tang, M. Qian, N. Liu, X.Z. Zhang, G.Y. Yang, and J. Wang, *JOM*, 67(3), 555 (2015). https://doi.org/10.1007/s11837-015-1300-4.
28. O.A. Quintana and W. Tong, *JOM*, 69(12), 2693 (2017). https://doi.org/10.1007/s11837-017-2590-5.
29. V.V. Popov, A. Katz-Demyanetz, A. Garkun, and M. Bamberger, *Addit. Manuf.*, 22(June), 834 (2018). https://doi.org/10.1016/j.addma.2018.06.003.
30. M. Velasco-Castro, E. Hernández-Nava, I.A. Figueroa, I. Todd, and R. Goodall, *Heliyon*, (2019). https://doi.org/10.1016/j.heliyon.2019.e02813.
31. C. Pauzon, K. Dietrich, P. Foret, S. Dubiez-LeGoff, E. Hryha, and G. Witt, *Addit. Manuf.*, (2020). https://doi.org/10.1016/j.addma.2020.101765.
32. K. Dietrich, J. Diller, S. Dubiez-Le Goff, D. Bauer, P. Forêt, and G. Witt, *Addit. Manuf.*, 32, 2020 (2019). https://doi.org/10.1016/j.addma.2019.100980.
33. G. Lindwall, P. Wang, U.R. Kattner, and C.E. Campbell, *JOM*, 70(9), 1692 (2018). https://doi.org/10.1007/s11837-018-3008-8.
34. B.E. Carroll, T.A. Palmer, and .M. Beese, *Acta Mater.*, 87, 309 (2015). https://doi.org/10.1016/j.actamat.2014.12.054.
35. ASTM F2924-14, *ASTM Standards* (2014). https://doi.org/10.1520/F2924-14.2.
36. ASTM F3001-14, . *ASTM Standards* (2014). https://doi.org/10.1520/F3001-14.
37. I.E. Anderson, E.M. White, and R. Dehoff, *Curr. Opin. Solid State Mater. Sci.*, 22(1), 8 (2018). https://doi.org/10.1016/j.cossms.2018.01.002.
38. J.A. Slotwinski, E.J. Garboczi, P.E. Stutzman, C.F. Ferraris, S.S. Watson, and M.A. Peltz, *J. Res. Natl. Instit. Stand. Technol.*, 119, 460 (2014). https://doi.org/10.6028/jres.119.018.
39. G. Jacob, A. Donmez, J. Slotwinski, and S. Moylan, *Meas. Sci. Technol.*, 27, 11 (2016). https://doi.org/10.1088/0957-0233/27/11/115601.
40. AMS4999, Titanium Alloy Laser Deposited Product 6Al - 4V Annealed. SAE International (2016).
41. ASTM F136-08, *ASTM Standards ((Superseded))* (2008). https://doi.org/10.1520/F0136-08E01.2.
42. ASTM F1472-08, *ASTM Standards ((Superseded))* (2008). https://doi.org/10.1520/F1472-08E01.2.
43. ASTM F1108-04, *ASTM Standards* ((Superseded)) (2009). https://doi.org/10.1520/F1108-04R09.2.
44. ASTM F136-13, *ASTM Standards* (2013). https://doi.org/10.1520/F0136-13.2.
45. ASTM F1108-14, *ASTM Standards* (2014). https://doi.org/10.1520/F1108-14.2.
46. ISO 17025, ISO Standards (Revised in 2017) (2005).
47. S.M. Gaytan, L.E. Murr, F. Medina, E. Martinez, M.I. Lopez, and R.B. Wicker, *Mater. Technol.*, 24(3), 180 (2009). https://doi.org/10.1179/106678509X12475882446133.
48. A. Mohammadhosseini, D. Fraser, S.H. Masood, and M. Jahedi, *Appl. Mech. Mater.*, 541–542, 160 (2014). https://doi.org/10.4028/www.scientific.net/AMM.541-542.160.
49. V. Petrovic and R. Niñerola, *Aircraft Eng. Aerospace Technol.*, 87(2), 147 (2015). https://doi.org/10.1108/AEAT-11-2013-0212.
50. A. Strondl, O. Lyckfeldt, H. Brodin, and U. Ackelid, *JOM*, 67(3), 549 (2015). https://doi.org/10.1007/s11837-015-1304-0.
51. AMS4911N, Titanium Alloy, Sheet, Strip, and Plate 6Al - 4V Annealed. SAE International (2014).
52. AMS4911R, Titanium Alloy, Sheet, Strip, and Plate 6Al - 4V Annealed. SAE International (2019).
53. ASTM E1941-10, *ASTM Standards* (2016). https://doi.org/10.1520/E1941-10.2.
54. ASTM E1447-09, *ASTM Standards ((Reapproved 2016))* (2009). https://doi.org/10.1520/E1447-09R16.2.
55. ASTM E1409-13, *ASTM Standards* (2013). https://doi.org/10.1520/E1409.
56. ASTM E2371-13, *ASTM Standards* (2013). https://doi.org/10.1520/E2371-13.2.
57. ASTM B215-15, *ASTM Standards* (2015). https://doi.org/10.1520/B0215-10.2.
58. ISO 22963:2008, Titanium and titanium alloys—Determination of oxygen—Infrared method after fusion under inert gas. ISO Standards (2008). https://www.iso.org/standard/41255.html.
59. P. Nandwana, W.H. Peter, R.R. Dehoff, L.E. Lowe, M.M. Kirka, F. Medina, and S.S. Babu, *Metall. Mater. Trans. B*, 47B(February), 754 (2016).
60. ASTM E 23-16b, *ASTM Standards* (2016). https://doi.org/10.1520/E0023-12C.2.
61. ASTM E23-18, *ASTM Standards* (2018). https://doi.org/10.1520/E0023-18. www.astm.org.
62. C. Wei, X. Ma, X. Yang, M. Zhou, C. Wang, Y. Zheng, W. Zhang, and Z. Li,*Mater. Lett.*, 221, 111 (2018). https://doi.org/10.1016/j.matlet.2018.03.124.
63. Y. Sun, M. Aindow, and R.J. Hebert, *Addit. Manuf.*, 21(2017), 544 (2018). https://doi.org/10.1016/j.addma.2018.02.011.
64. Y. Sun, M. Aindow, R.J. Hebert, *Mater. High Temp.*, 35(1–3), 217 (2018). https://doi.org/10.1080/09603409.2017.1389133.
65. R.P. Elliott, Diffusion in Titanium and Titanium Alloys. Air Force Technical Documentary Report ASD-TDR-62-561 (1962).
66. M. Yan, M.S. Dargusch, T. Ebel, and M. Qian, *Acta Mater.*, 68, 196 (2014). https://doi.org/10.1016/j.actamat.2014.01.015.
67. S. Chandrasekar, J.B. Coble, S. Yoder, P. Nandwana, R.R. Dehoff, V.C. Paquit, and S.S. Babu, *Addit. Manuf.*, (2020). https://doi.org/10.1016/j.addma.2019.100994.
68. Y. Cao, M. Delin, F. Kullenberg, and L. Nyborg, *Surf. Interface Anal.*, (2020). https://doi.org/10.1002/sia.6847.
69. G. Shanbhag and M. Vlasea, *Manuf. Lett.*, (2020). https://doi.org/10.1016/j.mfglet.2020.07.007.
70. A. Montelione, S. Ghods, R. Schur, C. Wisdom, D. Arola, and M. Ramulu, *Addit. Manuf.*, 35(2019), 1012016 (2020). https://doi.org/10.1016/j.addma.2020.101216.
71. R. Schur, S. Ghods, E. Schultz, C. Wisdom, R. Pahuja, A. Montelione, D. Arola, and M. Ramulu, *J. Failure Anal. Prevent.*, (2020). https://doi.org/10.1007/s11668-020-00875-0.
72. S. Ghods, E. Schultz, C. Wisdom, R. Schur, R. Pahuja, A. Montelione, D. Arola, and M. Ramulu, *Materialia*, 9(2019), 100631 (2020). https://doi.org/10.1016/j.mtla.2020.100631.
73. V. Seyda, N. Kaufmann, and C. Emmelmann, *Phys. Proc.*, 39, 425 (2012). https://doi.org/10.1016/j.phpro.2012.10.057.

74. R. O'Leary, R. Setchi, P. Prickett, G. Hankins, and N. Jones, An Investigation into the Recycling of Ti-6Al-4V Powder Used Within SLM to Improve Sustainability. SDM2015: 2nd International Conference on Sustainable Design and Manufacturing, (2015) pp. 14–17 (2015).
75. L. Grainger, *Investigating the Effects of Multiple Re-Use of Ti6Al4V Powder in Additive Manufacturing (AM)* (Renishaw Pp, White Paper, 2016), pp. 1–10.
76. K. Thejane, S. Chikosha, and W.B. du Preez, *South African J. Ind. Eng.*, 28(3Spec. Edn), 161 (2017). https://doi.org/10.7166/28-3-1853.
77. O.A. Quintana, J. Alvarez, R. Mcmillan, W. Tong, and C. Tomonto, *JOM*, 70(9), 1863 (2018). https://doi.org/10.1007/s11837-018-3011-0.
78. ASTM B822-17, *ASTM Standards* (2017). https://doi.org/10.1520/B0822-17.2.
79. ASTM B213-17, *ASTM Standards* **Superseded** (2017). https://doi.org/10.1520/B0213-17.2.
80. ASTM B527-15, *ASTM Standards* **Superseded** (2015). https://doi.org/10.1520/B0527-15.2.
81. ASTM B213-20, *ASTM Standards* (2020). https://doi.org/10.1520/B0964-16.2.
82. ASTM B527-20, *ASTM Standards* (2020). https://doi.org/10.1520/B0527-15.2.
83. ASTM E8/E8M-16a, *ASTM Standards* (2016). https://doi.org/10.1520/E0008.
84. P.E. Carrion, A. Soltani-Tehrani, S.M. Thompson, and N. Shamsaei, Effect of powder degradation on the fatigue behavior of additively manufactured as-built Ti-6Al-4V. Solid Freeform Fabrication 2018: Proceedings of the 29th Annual International Solid Freeform Fabrication Symposium - An Additive Manufacturing Conference pp. 1366–1372 (2018).
85. P.E. Carrion, A. Soltani-Tehrani, N. Phan, and N. Shamsaei, *JOM*, 71(3), 963 (2019). https://doi.org/10.1007/s11837-018-3248-7.
86. L. Denti, A. Sola, S. Defanti, C. Sciancalepore, and F. Bondioli, *Manuf. Technol.*, 19(2), 190 (2019).
87. L. Cordova, M. Campos, and T. Tinga, *JOM*, 71(3), 1062 (2019). https://doi.org/10.1007/s11837-018-3305-2.
88. F.J. Alamos, J. Schiltz, K. Kozlovsky, R. Attardo, C. Tomonto, T. Pelletiers, and S.R. Schmid, *Int. J. Refr. Metals Hard Mater.*, 91(2019), 105237 (2020). https://doi.org/10.1016/j.ijrmhm.2020.105273.
89. D. Gaskell, *Introduction to Metallurgical Thermodynamics*, 2nd edn. (London: Hemisphere, 1981).
90. V.L. Stout and M.D. Gibbons, *J. Appl. Phys.*, 26(12), 1488 (1955). https://doi.org/10.1063/1.1721936.
91. R.L. Stow, *Nature*, 184, 542 (1959).
92. K. Naito, T. Tsuji, T. Matsui, and K. Une, *J. Nuclear Sci. Technol.*, 11(1), 22 (1974). https://doi.org/10.1080/18811248.1974.9730608.
93. N.P. Kherani and W.T. Shmayda, *Fusion Technol.*, 8(2P2), 2399 (1985).
94. P. Kofstad, *J. Less-Common Metals*, 12(6), 449 (1967). https://doi.org/10.1016/0022-5088(67)90017-3.
95. G.E. Camargo, *Revista Materia*, 12(3), 525 (2007).
96. J. Stringer, *Acta Metall.*, 8(11), 758 (1960). https://doi.org/10.1021/j100885a024.
97. J. Unnam, R.N. Shenoy, and R.K. Clark, *Oxidat. Metals*, 26(3/4), 231 (1986).
98. H. Guleryuz and H. Cimenoglu, *J. Alloys Comp.*, 472(1–2), 241 (2009). https://doi.org/10.1016/j.jallcom.2008.04.024.
99. F. Motte, C. Coddet, P. Sarrazin, M. Azzopardi, and J. Besson, *Oxidat. Metals*, 10(2), 113 (1976). https://doi.org/10.1007/BF00614241.
100. M.N. Mungole, N. Singh, and G.N. Mathur, *Mater. Sci. Technol.*, 18(1), 111 (2002). https://doi.org/10.1179/026708301125000302.
101. Y. Wouters, A. Galerie, and J.P. Petit, *Solid State Ionics*, 104(1–2), 89 (1997). https://doi.org/10.1016/s0167-2738(97)00400-1.
102. J. Whiting and J. Fox, Characterization of feedstock in the powder bed fusion process: Sources of variation in particle size distribution and the factors that influence them. Solid Freeform Fabrication 2016: Proceedings of the 27th Annual International Solid Freeform Fabrication Symposium—An Additive Manufacturing Conference, SFF 2016 pp. 1057–1068 (2016).
103. C. Schade and G.K.N. Hoeganaes, *Powder Metall.*, 7, 88 (2015). https://doi.org/10.31399/asm.hb.v07.a0006088.
104. Y.F. Yang, S.D. Luo, G.B. Schaffer, and M. Qian, *Mater. Sci. Eng. A*, 573, 166 (2013). https://doi.org/10.1016/j.msea.2013.02.042.
105. M. Yan, Y. Liu, G.B. Schaffer, and M. Qian, *Scr. Mater.*, 68(1), 63 (2013). https://doi.org/10.1016/j.scriptamat.2012.09.024.